

# We are IntechOpen, the world's leading publisher of Open Access books Built by scientists, for scientists

6,900

Open access books available

186,000

International authors and editors

200M

Downloads

Our authors are among the

154

Countries delivered to

TOP 1%

most cited scientists

12.2%

Contributors from top 500 universities



WEB OF SCIENCE™

Selection of our books indexed in the Book Citation Index  
in Web of Science™ Core Collection (BKCI)

Interested in publishing with us?  
Contact [book.department@intechopen.com](mailto:book.department@intechopen.com)

Numbers displayed above are based on latest data collected.  
For more information visit [www.intechopen.com](http://www.intechopen.com)



# Magnetic Assembly and Functionalization of One-Dimensional Nanominerals in Optical Field

*Meng Fu, Zepeng Zhang, Rui Jiang and Hongbao Liu*

## Abstract

Magnetic particles can be oriented along the magnetic field direction to achieve orderly arrangement under the magnetic field. Optical functional materials such as photonic crystal and liquid crystal can be obtained according to magnetic induced ordered nanostructure assembly. One-dimensional natural clay minerals with unique structure, composition and properties can be used as structural base to prepare anisotropic magnetic nanoparticles by decorated with magnetic particles, achieving unique optical functional properties. In this chapter, one-dimensional clay minerals@Fe<sub>3</sub>O<sub>4</sub> nanocomposites were prepared by co-precipitation. The resulting one-dimensional clay minerals@Fe<sub>3</sub>O<sub>4</sub> nanocomposites are superparamagnetic. They can be oriented along the direction of the magnetic field and produce an instantaneously reversible response. These magnetic mineral materials can be dispersed in a dilute acid solution to form stable colloid solutions. These stable colloid solutions produce a similar magnetically controlled liquid crystal with Bragg diffraction under an external magnetic field. Their optical properties are affected by magnetic field intensity, magnetic field direction and solid content. The results show that the functionalization of one-dimensional clay minerals has potential applications in display devices, photonic switches and other fields.

**Keywords:** One-dimensional clay minerals, magnetic assembly, magnetically controlled liquid crystal, photonic crystal

## 1. Introduction

The pursuit of nanomineral functional materials with novel properties and improved performance is a continually expanding research area that covers chemistry, physics, biology and materials science. It is an important research direction in the field of mineral functional materials to explore, develop and apply the electrical, optical, magnetic, acoustic and thermal properties of natural minerals and rocks, especially to study and prepare mineral functional materials with electrical, optical, magnetic, acoustic and thermal properties by using the unique structure, composition and morphology of natural minerals. Among the various explored nanostructures, the study of one-dimensional (1D) nanominerals such as wires, rods, and tubes has entered a period of fast development within the past several

years, and is presently the focus of many research groups [1–3]. Considering that magnetic nanoparticles can be controlled reversibly by the magnetic field, superparamagnetic  $\text{Fe}_3\text{O}_4$  nanoparticles can be coated on the surface of the anisotropic 1D clay minerals to realize the magnetic field induced anisotropic ordered orientation and form liquid crystal phase. In recent years, research efforts have been directed on the one-dimensional nanominerals coated or assembled with magnetic nanoparticles [4–7]. The research on the magnetic response and optical properties of magnetic mineral composites is helpful to improve the added value of natural mineral materials, develop mineral functional materials with special optical and magnetic properties, and accelerate the development of mineral industry.

In this chapter, one-dimensional natural nano-clay-minerals with unique structures, compositions and properties have been used as structural base to prepare anisotropic magnetic one-dimensional nanomaterials by decorated one-dimensional natural nano-clay-minerals with magnetic particles. Magnetic particles can be oriented along the magnetic field direction to achieve orderly arrangement under the magnetic field. Optical functional materials with unique optical functional properties such as photonic crystal and liquid crystal have been obtained according to magnetic induced ordered nanostructure assembly. All the related research progress our research group made are summarized as well as existing problems and prospects of the future application and development direction.

## 2. Raw material

Clay mineral is the main component of clay rock and soil, which is a kind of rich non-metallic mineral resources on the earth. In recent years, people have been constantly studying the structure and properties of clay minerals, and exploring the composite of clay minerals and other materials, in order to expect that the composite materials will make a breakthrough in the field of deep processing and application of non-metallic minerals, and also obtain a series of research results. In these studies, the research objects mainly include layered silicate minerals represented by montmorillonite group, kaolinite group, illite group, vermiculite group, and fibrous silicate minerals represented by sepiolite group [8]. Attapulgite and sepiolite are typical one-dimensional nanominerals. Their research direction and content are also very representative. In recent years, researchers at home and abroad mainly focus on the following aspects: ① as adsorbents [9], they can adsorb heavy metal ions or pollutants; ② As a carrier, it catalyzes other chemical reactions or provides a place for other reactions [10]; ③ When clay minerals are compounded with other polymers or organic materials, the mechanical properties, thermal stability, flame retardancy and barrier properties of the materials can be significantly improved [11]; ④ As catalyst of reaction [12]; ⑤ As a rheological control agent, it is used in oil-based drilling fluid [13]; In addition, the two minerals also have a lot of research and application in animal husbandry, medicine and so on. Here, attapulgite and sepiolite will be taken as examples to introduce the structure and properties of one-dimensional clay minerals.

### 2.1 Attapulgite

In this chapter, we use attapulgite (short crystal rod) as the research object. Wang Aiqin et al. [14] pointed out in “*Attapulgite rod bundle dissociation and its nano functional composites*” that the products of hydrothermal alteration have soft appearance, good crystallinity and long fiber, which are usually called palygorskite; However, the sedimentary products are characterized by dense appearance, poor

crystallization performance, short crystal rod and high iron content, which are called attapulgite. In the following content, we will use the naming principle mentioned in “Attapulgite rod bundle dissociation and its nano functional composites” to unify these short rod minerals as attapulgite.

### 2.1.1 Crystal structure

The molecular formula of attapulgite is  $\text{Mg}_5[\text{Si}_4\text{O}_{10}]_2(\text{OH})_2 \cdot 8\text{H}_2\text{O}$ , which belongs to monoclinic system with space group C2/m (no.12);  $a = 13.24 \text{ \AA}$ ,  $b = 17.89 \text{ \AA}$ ,  $c = 5.21 \text{ \AA}$ ,  $\alpha = \gamma = 90^\circ$ ,  $\beta = 8^\circ$ ,  $Z = 2$  [15]. The crystal structure is shown in **Figure 1(a)**. A  $[\text{Mg}(\text{O}, \text{OH})_6]$  octahedron is sandwiched by two  $[\text{SiO}_4]$  tetrahedrons, forming a TOT type “I beam” with one-dimensional infinite extension along the c-axis, and its width is about  $18 \text{ \AA}$ . The adjacent TOT type “I beam” is staggered up and down, forming a wide channel along the c-axis at the position of inert oxygen, which is about  $3.7 \text{ \AA} \times 6.4 \text{ \AA}$ . The channel is filled with water molecules. There are three forms of water in attapulgite, one is structural water hydroxyl, the second is crystal water coordinated with octahedral cation, the third is zeolite water connected by hydrogen bond in the channel. The  $[\text{SiO}_4]$  tetrahedron by a common edge forms a six membered ring at the same height, and the  $[\text{Mg}(\text{O}, \text{OH})_6]$  octahedron is also joined into a layer by a common edge, so attapulgite has both chain and layered structure.

### 2.1.2 Microstructure and physicochemical properties

**Figure 1(e)** and **(f)** show the size distribution histograms of these monodisperse attapulgite nanocrystals counted from **Figure 1(b)** [16]. The average length and width of attapulgite rods are  $0.85 \mu\text{m}$  and  $63 \text{ nm}$ , respectively.

The color of attapulgite is white, gray or light brown with glass luster, hardness of 2–3, specific gravity of 2.05–2.32, a sense of smoothness [15]. It has viscosity and plasticity, strong water absorption, no expansion in water. Because of isomorphism, the surface of attapulgite is negatively charged, and it has cation exchange performance, but lower than that of montmorillonite. It has a strong adsorption function, because the wide channels in the crystal structure greatly increase the specific surface area of attapulgite.

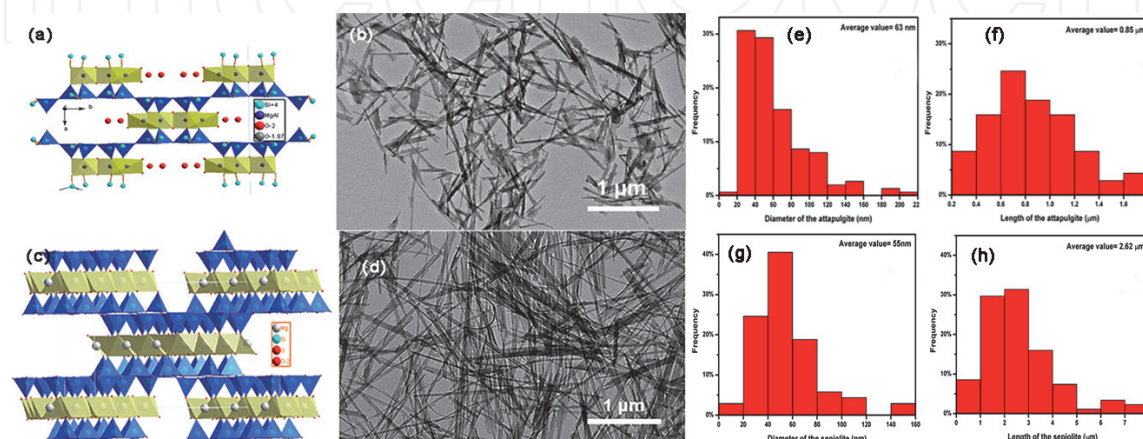


**Figure 1.** Raw materials: (a) the crystal structure of attapulgite; (b) the microstructure of attapulgite in TEM; (c) the crystal structure of Sepiolite; (d) the microstructure of sepiolite in TEM; distribution histograms: (e) diameter of attapulgite; (f) length of attapulgite; (g) diameter of sepiolite; (h) length of sepiolite.



## 2.2 Sepiolite

### 2.2.1 Crystal structure

The molecular formula of sepiolite is  $\text{Mg}_8[\text{Si}_6\text{O}_{15}]_2(\text{OH})_4 \cdot 12\text{H}_2\text{O}$ , which belongs to orthorhombic system with space group Pncn (no.52);  $a = 13.40 \text{ \AA}$ ,  $b = 36.80 \text{ \AA}$ ,  $c = 5.28 \text{ \AA}$ ,  $\alpha = \gamma = \beta = 90^\circ$ ,  $Z = 2$  [15]. The crystal structure is shown in **Figure 1(c)**, which is basically similar to that of attapulgite. The difference is that the Mg and  $\text{H}_2\text{O}$  content of sepiolite is higher than that of attapulgite; Structurally, the TOT type “I-beam” width of sepiolite is larger, about  $27 \text{ \AA}$ ; The cross-sectional area of through passage is also larger than that of attapulgite, about  $3.7 \text{ \AA} \times 10.6 \text{ \AA}$ .

### 2.2.2 Microstructure and physicochemical properties

**Figure 1(g)** and **(h)** shows the size distribution histograms of these monodisperse sepiolite nanocrystals counted from **Figure 1(d)**. The average length and width of sepiolite fibers are  $2.6 \mu\text{m}$  and  $55 \text{ nm}$ , respectively [16]. Compared with the size of attapulgite, sepiolite has higher aspect ratio.

Sepiolite is usually white, light gray or maroon, also has glass luster, hardness of 2–3, specific gravity of 2–2.5, with a sense of smoothness, soft texture [15]. Since the similar crystal structure with attapulgite, sepiolite has negative charge on its surface, and its cation exchange properties, large specific surface area, good adsorption property are similar to those of attapulgite.

## 3. Magnetic assembly of one-dimensional nanominerals

### 3.1 Construction of one-dimensional clay mineral magnetic materials

The magnetic particles coated on the surface of one-dimensional clay minerals can bring magnetism to non-magnetic one-dimensional clay minerals. The most common method to load magnetic particles on clay mineral surface is to synthesize  $\text{Fe}_3\text{O}_4$  nanoparticles in solution with clay minerals as dispersed phase. The  $\text{Fe}_3\text{O}_4$  nanoparticles cannot be coated uniformly on the one-dimensional clay surface minerals is the main problem. There are many methods for the synthesis of  $\text{Fe}_3\text{O}_4$ , including co-precipitation, thermal solvent and so on. A lot of literature shows that the synthesis method of  $\text{Fe}_3\text{O}_4$  has no obvious influence on the uniform coating on the carrier. The surface morphology and crystal defects of the carrier, the active functional groups on the carrier surface, the affinity between the carrier and  $\text{Fe}_3\text{O}_4$ , suitable heterogeneous nucleation environment have a decisive influence on the uniform coating of the carrier. In this section, the magnetic assembly process of one-dimensional clay minerals (as shown in **Figure 2**) will be described by co-precipitation method. The first is to modify one-dimensional clay minerals by modifier, which helps clay minerals evenly disperse in the solution, and at the same time, it can also bring more active functional groups to clay minerals surface and help deposit  $\text{Fe}_3\text{O}_4$  uniformly on the surface of clay minerals. The second is the uniform coating of  $\text{Fe}_3\text{O}_4$  on the surface of one-dimensional clay minerals. When  $\text{Fe}_3\text{O}_4$  nanoparticles are deposited on the surface of one-dimensional clay minerals, the control of heterogeneous nucleation conditions is very important. Influence factors, including suitable surface adhering surfactants, modifier concentration,  $\text{Fe}^{2+}/\text{Fe}^{3+}$  concentration, temperature etc. affect the uniform deposition and particle diameter of  $\text{Fe}_3\text{O}_4$  on the surface of clay minerals by influencing the homogeneous nucleation rates, heterogeneous nucleation rates and particle growth rate.

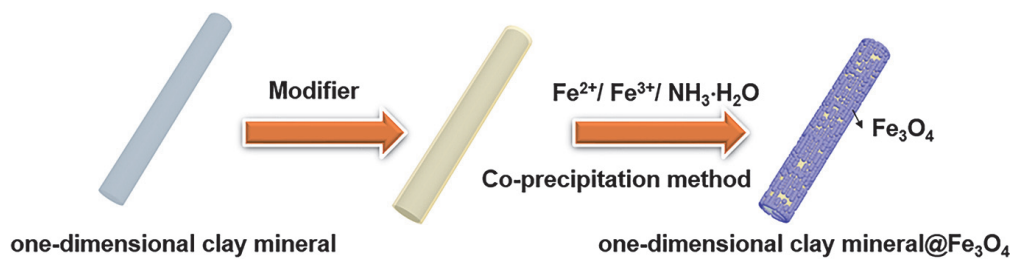


**Figure 2.**  
Magnetic coating of one dimensional nano clay minerals.

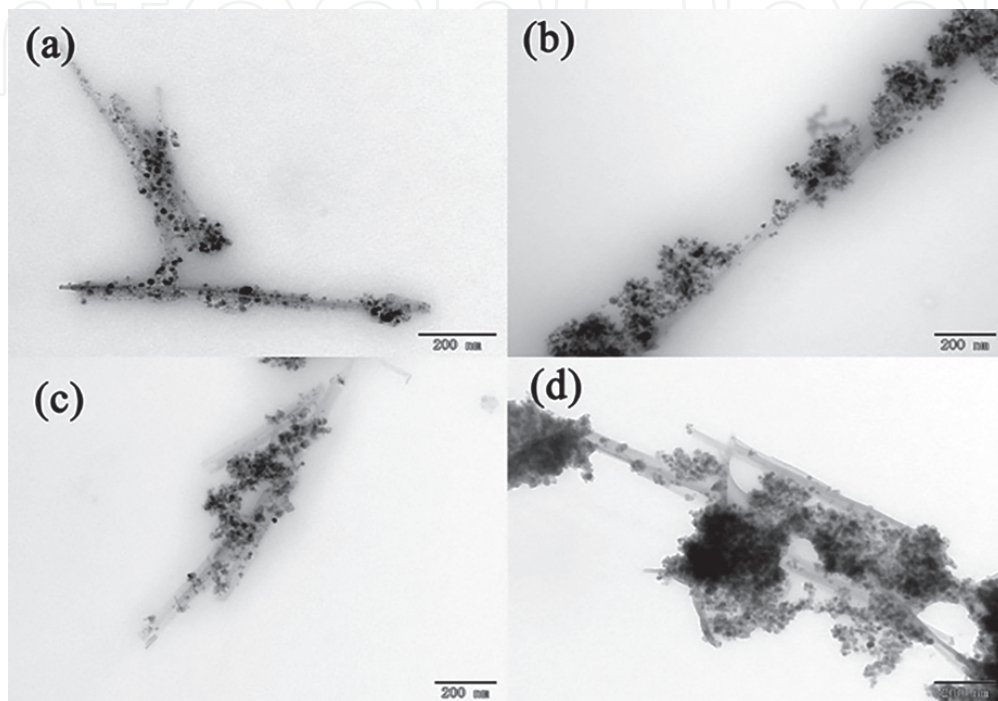


**Figure 3.**  
TEM images of attapulgites- $\text{Fe}_3\text{O}_4$  one-dimensional nanocomposites synthesized (no surfactant) with different concentrations of  $\text{FeCl}_3 \cdot 6\text{H}_2\text{O}$ : (a) 0.01 mmol/L; (b) 0.02 mmol/L; (c) 0.03 mmol/L; (d) 0.04 mmol/L.

### 3.2 Influence factor of one-dimensional clay mineral magnetic assembly

#### 3.2.1 Surface modification of one-dimensional nanominerals

Uniform  $\text{Fe}_3\text{O}_4$  shell decorated on the surface is not available while no surface pretreatments were carried out to introduce new surface functional groups.  $\text{Fe}_3\text{O}_4$  microspheres or irregular islands will grow onto the surface of 1D nanominerals (**Figure 3**) [17], which may be attributed to a significantly different crystalline structure in lattice symmetry and lattice constant between  $\text{Fe}_3\text{O}_4$  and 1D nanominerals as well as the amorphization of natural mineral. Only by modifying the surface of non-magnetic 1D nanomineral and improving the surface affinity between 1D nanomineral and  $\text{Fe}_3\text{O}_4$ , can the uniform growth or uniform assembly of magnetic particles on the 1D nanomineral surface be promoted. Modification methods include inorganic modification and organic modification.

##### 3.2.1.1 Inorganic modification

Inorganic modifiers HCl and  $\text{H}_2\text{O}_2$  are often used to modify nanominerals.

The TEM images of acid treated attapulgite@ $\text{Fe}_3\text{O}_4$  were illustrated in **Figure 4**. Compared to the growth of  $\text{Fe}_3\text{O}_4$  nanoparticles on the raw attapulgite (**Figure 3**),

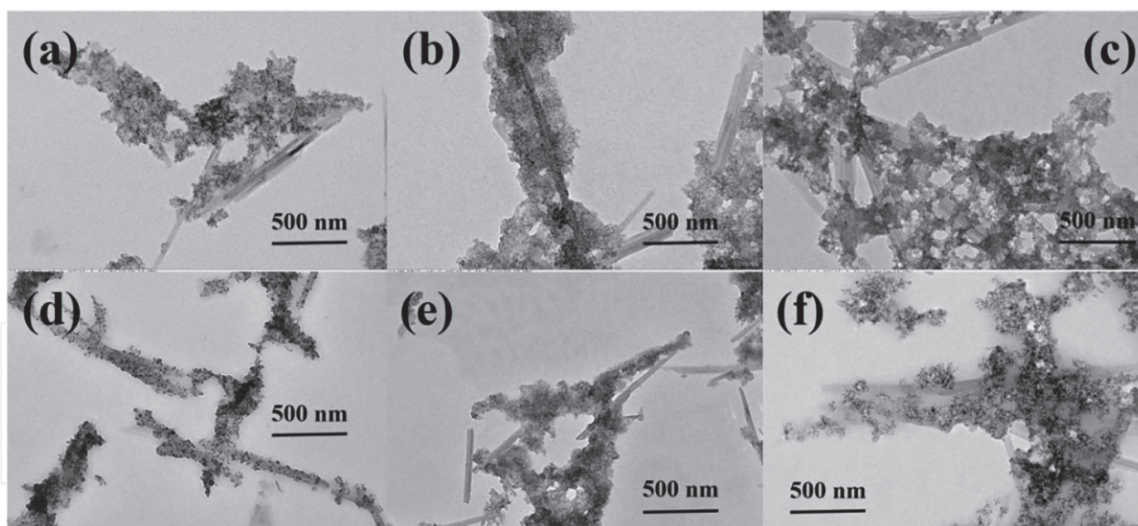


**Figure 4.**

The TEM images of acid treated attapulgite@Fe<sub>3</sub>O<sub>4</sub> with different acid concentrations (a) 0.5 Mol·L<sup>-1</sup>; (b) 1.0 Mol·L<sup>-1</sup>; (c) 1.5 Mol·L<sup>-1</sup>; (d) 2.0 Mol·L<sup>-1</sup>; (e) 2.5 Mol·L<sup>-1</sup>; (f) 3.0 Mol·L<sup>-1</sup>.

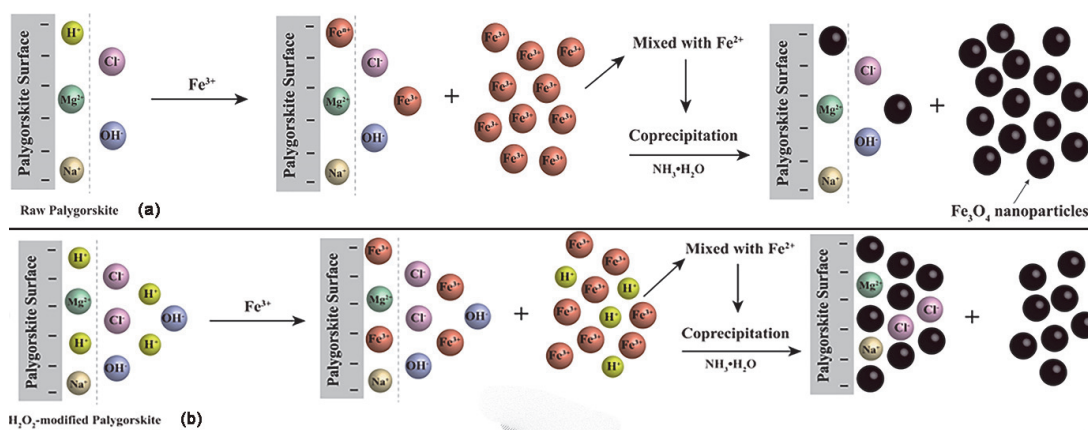


**Figure 5.**

Proposed growth mechanism of Fe<sub>3</sub>O<sub>4</sub> nanoparticles on (a) acid-modified attapulgite/palygorskite; (b) H<sub>2</sub>O<sub>2</sub>-modified attapulgite/palygorskite.

the acid modification was found to help Fe<sub>3</sub>O<sub>4</sub> nanoparticles adhere on the surface of attapulgite [18]. It could be observed from **Figure 4** that when the HCl concentration was 2.0 mol·L<sup>-1</sup>, the Fe<sub>3</sub>O<sub>4</sub> nanoparticles on modified attapulgite surface were the most uniform.

It is well known that one-dimensional clay mineral has zeolite-like channels and exchangeable cations such as Na<sup>+</sup>, K<sup>+</sup>, and Mg<sup>2+</sup>, which allows H<sup>+</sup> to interact with the mineral. While H<sup>+</sup> cations attached on the surface of one-dimensional clay mineral, the Si-O bonds were corroded and Al<sup>3+</sup> or Mg<sup>2+</sup> cations in octahedron were displaced by H<sup>+</sup> cations to expose more negative active sites, so that more H<sup>+</sup> cations could absorb on attapulgite surface and the Cl<sup>-</sup> ions continuously gravitated to H<sup>+</sup> via electrostatic attraction. The new electric double layer was formed on the modified one-dimensional clay mineral surface (as shown in the **Figure 5(a)**), resulting in the increase of zeta potential absolute values. Besides, the impurities in the one-dimensional clay mineral channels such as carbonate, amorphous silica etc. were dissolved so that the channels were cleared, leading to the increase of specific surface area. With the absolute values of Zeta Potential and specific surface area enlargement, the acid modified one-dimensional clay mineral could absorb more Fe<sup>3+</sup>/Fe<sup>2+</sup> cations. When FeCl<sub>3</sub> was added into the modified one-dimensional clay mineral suspension, Fe<sup>3+</sup> cations would replace H<sup>+</sup> ions absorbed on one-



dimensional clay mineral surface, then  $H^+$  ions were released into solution. Once  $NH_3 \cdot H_2O$  was added into the system, many  $Fe_3O_4$  nuclei were generated on the surface of attapulgite simultaneously in a short time, resulting in a dense  $Fe_3O_4$  shell composed of small  $Fe_3O_4$  nanoparticles with a mean size of about 10–30 nm.

The TEM images of  $H_2O_2$  treated attapulgite@ $Fe_3O_4$  were illustrated in **Figure 6** [18]. Compared to the growth of  $Fe_3O_4$  nanoparticles on the raw attapulgite (**Figure 3**), the attapulgite nanorods were covered more uniformly by  $Fe_3O_4$  nanoparticles. It could be observed from **Figure 6(d)** that when the  $H_2O_2$  concentration was 25%, the  $Fe_3O_4$  nanoparticles on modified attapulgite surface were the most uniform.  $H_2O_2$  can help one-dimensional clay mineral absorb more  $Fe^{3+}$  cations as shown in **Figure 5(b)**, thus depositing more evenly  $Fe_3O_4$  nanoparticles on the surface.

### 3.2.1.2 Organic modification

When modifying one-dimensional clay minerals with organic compound, the modifier is often selected according to the structural characteristics of one-dimensional clay minerals. For one-dimensional clay minerals with negative surface, cationic or poly-cationic modifiers are often used.

The effects of polyethylenimine (PEI) concentration on the morphology of the one-dimensional nanocomposites were examined by TEM and SEM and displayed in **Figure 7**. The left is TEM result and the right is SEM result [17]. The figure shows that when PEI is not added to the solution,  $Fe_3O_4$  adheres to the surface of attapulgite in the form of microsphere or island structure. The microsphere or island structure does not form close packing, and there are a lot of gaps between the microspheres. Therefore,  $Fe_3O_4$  cannot grow on the outer surface of attapulgite forming a uniform core-shell structure. It may be due to the lattice mismatch between  $Fe_3O_4$  and attapulgite. At the same time, the existence of a large number of amorphous regions on the surface of attapulgite brings the unreachable interface energy to the growth of  $Fe_3O_4$ . On the other hand, the surface inhomogeneity of natural attapulgite determines that different positions on the surface of attapulgite have different reactivity and position dependent interfacial tension. These factors make it difficult for  $Fe_3O_4$  to grow directly on the surface of attapulgite. When the PEI content is 0.1 mg/mL, there are still a lot of uncoated attapulgite. When the

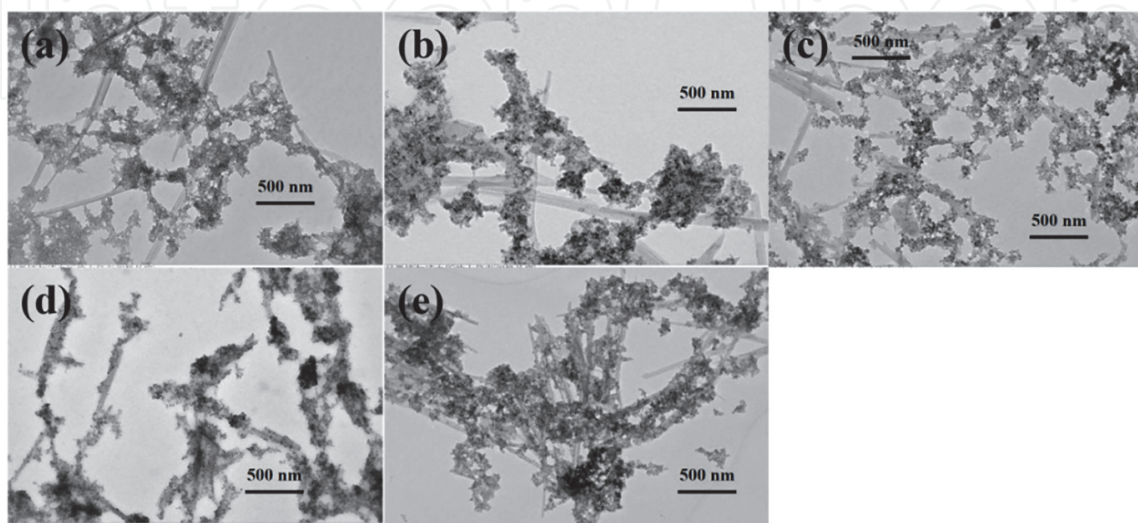


**Figure 6.**  
The TEM images of  $H_2O_2$  treated attapulgite@ $Fe_3O_4$  with different  $H_2O_2$  concentrations: (a) 10%; (b) 15%; (c) 20%; (d) 25%; (e) 30%.



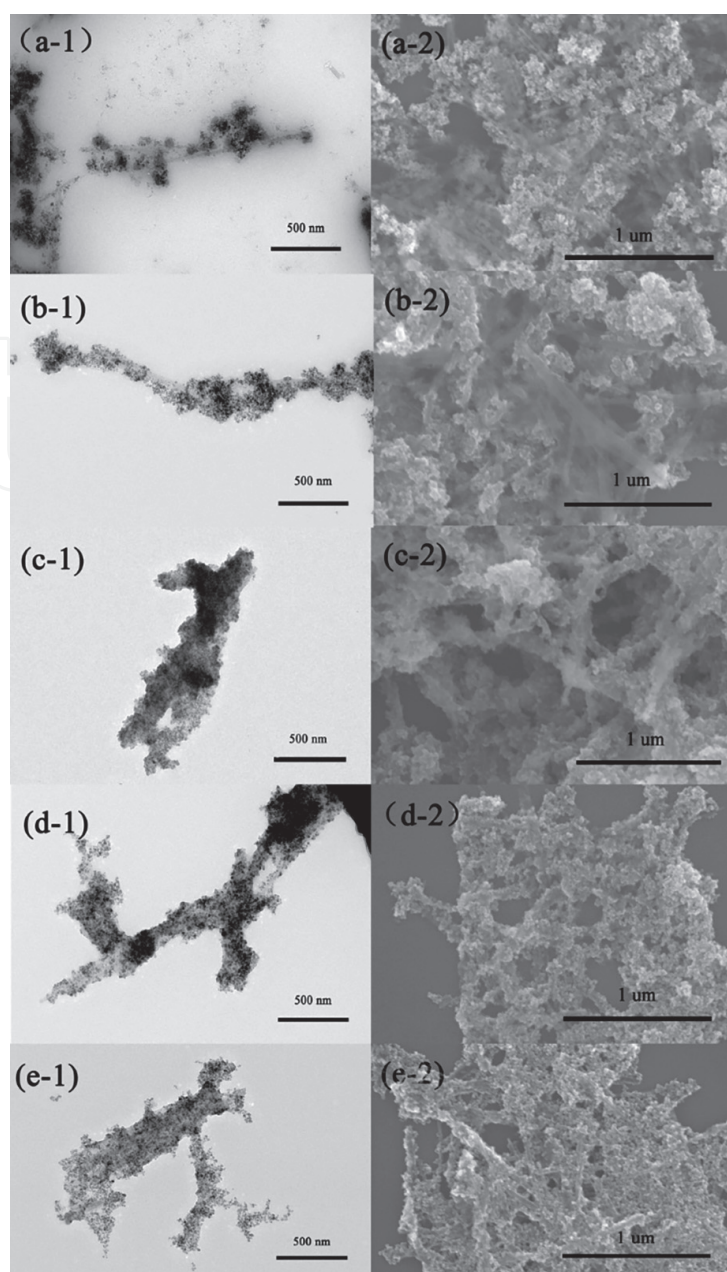


**Figure 7.**

*Images of attapulgites- $\text{Fe}_3\text{O}_4$  one-dimensional nanocomposites synthesized with different concentrations of PEI: TEM: (a-1) 0 mg/mL; (b-1) 0.1 mg/mL; (c-1) 0.2 mg/mL; (d-1) 0.5 mg/mL; (e-1) 1 mg/mL; SEM: (a-2) 0 mg/mL; (b-2) 0.1 mg/mL; (c-2) 0.2 mg/mL; (d-2) 0.5 mg/mL; (e-2) 1 mg/mL.*

amount of PEI is 0.2 mg/mL, more PEI is adsorbed on the surface of attapulgite, and PEI acts as a link to adsorb  $\text{Fe}^{3+}$  and  $\text{Fe}^{2+}$ . When alkali solution is added,  $\text{Fe}_3\text{O}_4$  particles are formed in situ on the surface of attapulgite, realizing 100% close packed coating of  $\text{Fe}_3\text{O}_4$  nanoparticles. When the PEI content was further increased (0.5 mg/mL or 1.0 mg/mL), the  $\text{Fe}_3\text{O}_4$  nanoparticles became smaller and no longer accumulated tightly on the surface of attapulgite. They dispersed evenly, even scattered into the solution. The results may be caused by the diffusion of high concentration PEI into the solution and the increase of the viscosity of the solution, which makes it difficult for  $\text{Fe}_3\text{O}_4$  particles to diffuse, move and form close packing. The growth of  $\text{Fe}_3\text{O}_4$  is accompanied by the adsorption of PEI in the solution, which prevents the growth of  $\text{Fe}_3\text{O}_4$  nanoparticles and leads to the formation of nanoparticles with small size. In conclusion, with the increase of PEI content,  $\text{Fe}_3\text{O}_4$  gradually dispersed and coated on the surface of attapulgite from island aggregation state, achieving uniform and compact coating. 0.2 mg/mL was the best PEI content for the formation of attapulgites@ $\text{Fe}_3\text{O}_4$  one-dimensional nanocomposites.

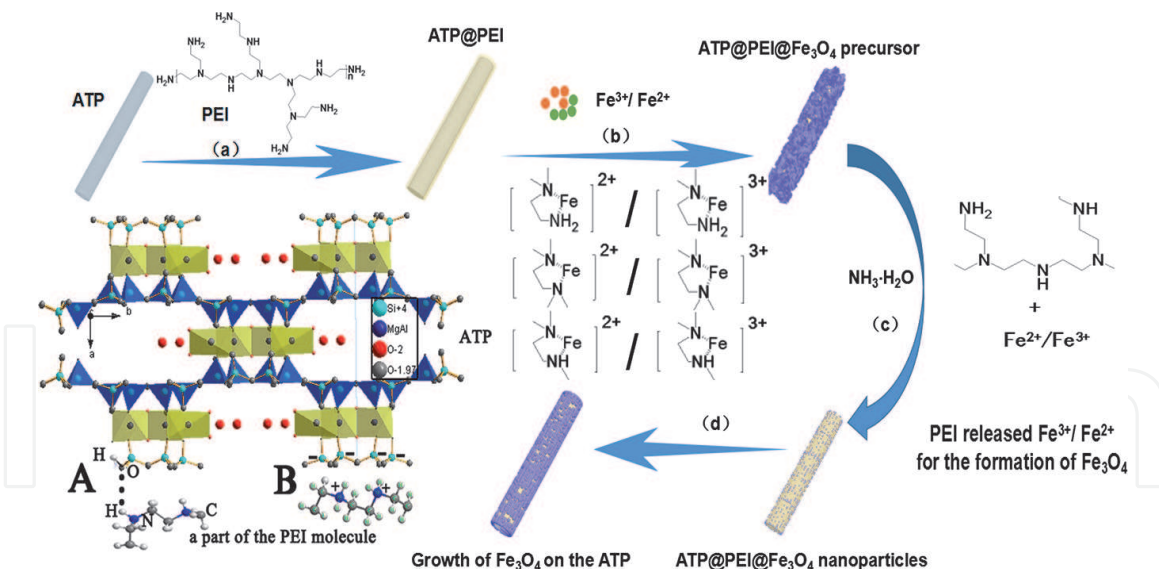


**Figure 8.**  
*Proposed scheme for the growth of uniform  $\text{Fe}_3\text{O}_4$  nanostructures on the surface of the one-dimensional clay minerals with PEI by co-precipitation method.*

The growth mechanism of uniform coating of  $\text{Fe}_3\text{O}_4$  on the surface of one-dimensional clay minerals is shown in **Figure 8**. Firstly, PEI is adsorbed on the surface of attapulgite by hydrogen bonding and electrostatic interaction. Then  $\text{Fe}^{3+}/\text{Fe}^{2+}$  was added to the system, and the PEI on the surface of attapulgite adsorbed  $\text{Fe}^{3+}/\text{Fe}^{2+}$  onto the surface of attapulgite through complexation by PEI. Stable five membered cyclic complexes can be formed between PEI and  $\text{Fe}^{3+}/\text{Fe}^{2+}$ , and iron salts are continuously accumulated to form the precursor of  $\text{Fe}_3\text{O}_4$ . With the addition of ammonia, a large number of  $\text{Fe}_3\text{O}_4$  nuclei are formed at the same time. At this time, PEI releases  $\text{Fe}^{3+}/\text{Fe}^{2+}$  for the in-situ formation and growth of  $\text{Fe}_3\text{O}_4$ . On the other hand, suitable temperature and iron salt concentration can promote the heterogeneous nucleation of  $\text{Fe}_3\text{O}_4$  on the surface of attapulgite. With the increase of time,  $\text{Fe}_3\text{O}_4$  nanoparticles move and diffuse on the surface of attapulgite to minimize the surface energy of the system, thus forming a one-dimensional composite. With the smallest particles dissolving and the larger ones growing up by Ostwald ripening, the attapulgites- $\text{Fe}_3\text{O}_4$  core-shell nanocomposites are obtained finally [17].

### 3.2.2 Effects of ferric salt concentration

The TEM and SEM results of attapulgites- $\text{Fe}_3\text{O}_4$  one-dimensional nanocomposites with different  $\text{FeCl}_3 \cdot 6\text{H}_2\text{O}$  content are shown in **Figure 9** [17]. The left side is TEM and the right side is SEM of corresponding samples. a/b/c/d is the sample with 0.01/ 0.02 / 0.03/ 0.04 mmol/L of  $\text{Fe}^{3+}$ . It can be seen from the figure that with the increase of iron salt content,  $\text{Fe}_3\text{O}_4$  on the surface of attapulgite changes from sparse dispersion to close packing (thickness: 10–20 nm), and finally becomes thicker (outer layer thickness: 30–40 nm). However, when the addition amount of  $\text{Fe}^{3+}$  reached 0.04 mmol/L, the inhomogeneous coating appeared again. Low supersaturation promotes heterogeneous nucleation of  $\text{Fe}_3\text{O}_4$  on the surface of attapulgite to obtain large nanoparticles; High supersaturation leads to similar homogeneous and heterogeneous nucleation rates and small nanoparticles. Therefore, when the concentration of  $\text{Fe}^{3+}$  exceeds the critical value, the relative supersaturation of  $\text{Fe}_3\text{O}_4$  is too large, resulting in the same rate of homogeneous nucleation and heterogeneous nucleation, small  $\text{Fe}_3\text{O}_4$  nanoparticles appear, and form a large number of nanoparticle aggregates, and finally incomplete coating

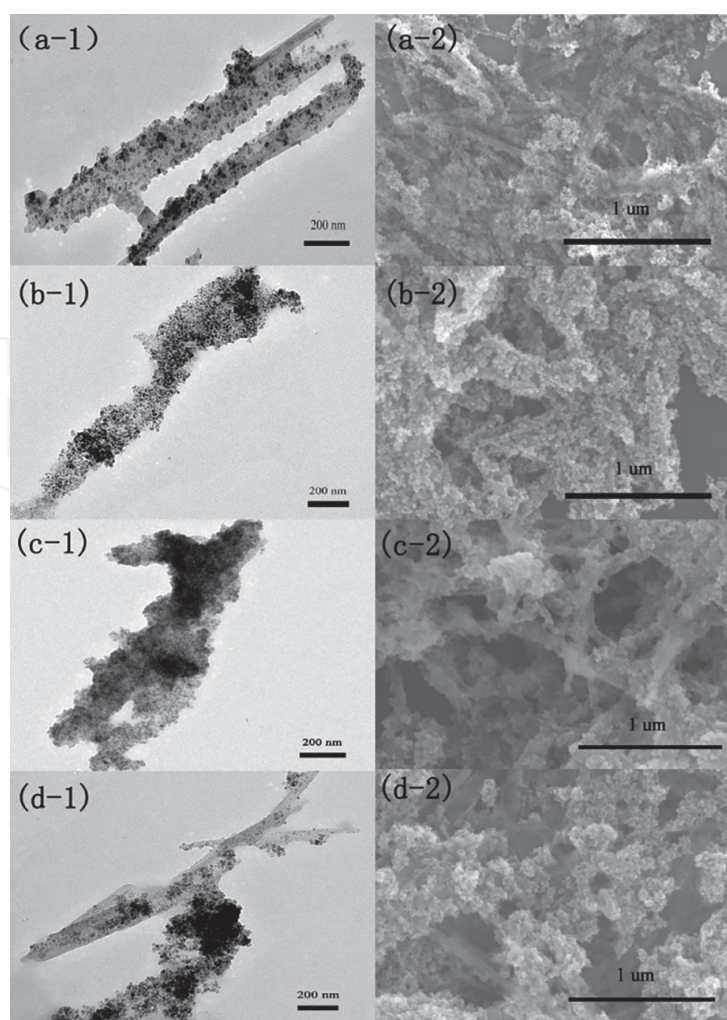


**Figure 9.**

Images of attapulgites- $\text{Fe}_3\text{O}_4$  one-dimensional nanocomposites synthesized with different concentrations of  $\text{FeCl}_3 \cdot 6\text{H}_2\text{O}$ : TEM: (a-1) 0.01 mmol/L; (b-1) 0.02 mmol/L; (c-1) 0.03 mmol/L; (d-1) 0.04 mmol/L; SEM: (a-2) 0.01 mmol/L; (b-2) 0.02 mmol/L; (c-2) 0.03 mmol/L; (d-2) 0.04 mmol/L.

results. It can be seen that the uniform coating of  $\text{Fe}_3\text{O}_4$  on the surface of attapulgite can be achieved when the concentration of  $\text{Fe}^{3+}$  does not exceed the critical concentration ( $< 0.04$  mmol/L), and the thickness of  $\text{Fe}_3\text{O}_4$  layer can be changed by changing amount of  $\text{Fe}_3\text{O}_4$ .

### 3.2.3 Effects of temperature

**Figure 10** shows the TEM and SEM of attapulgite@ $\text{Fe}_3\text{O}_4$  synthesized at different temperatures. a, b, c and d were  $40^\circ\text{C}$ ,  $60^\circ\text{C}$ ,  $80^\circ\text{C}$  and  $100^\circ\text{C}$  respectively. The figure shows that too high and too low temperature are not conducive to the uniform coating of  $\text{Fe}_3\text{O}_4$  on the surface of attapulgite. This is because the supersaturation of the solution is too high at low temperature, which leads to the same homogeneous nucleation rate with heterogeneous nucleation rate of  $\text{Fe}_3\text{O}_4$ . It makes  $\text{Fe}_3\text{O}_4$  aggregates instead of nucleating on the surface of attapulgite. Too high temperature will lead to too low relative supersaturation. Although it is conducive to heterogeneous nucleation, the nucleation rate of  $\text{Fe}_3\text{O}_4$  is low. The high temperature will also make  $\text{Fe}_3\text{O}_4$  particles move rapidly, forming some very thick  $\text{Fe}_3\text{O}_4$  coating and some completely uncoated attapulgite, which is not a very good coating effect. Therefore,  $60\text{--}80^\circ\text{C}$  is the most favorable temperature for the formation of attapulgite@ $\text{Fe}_3\text{O}_4$ .



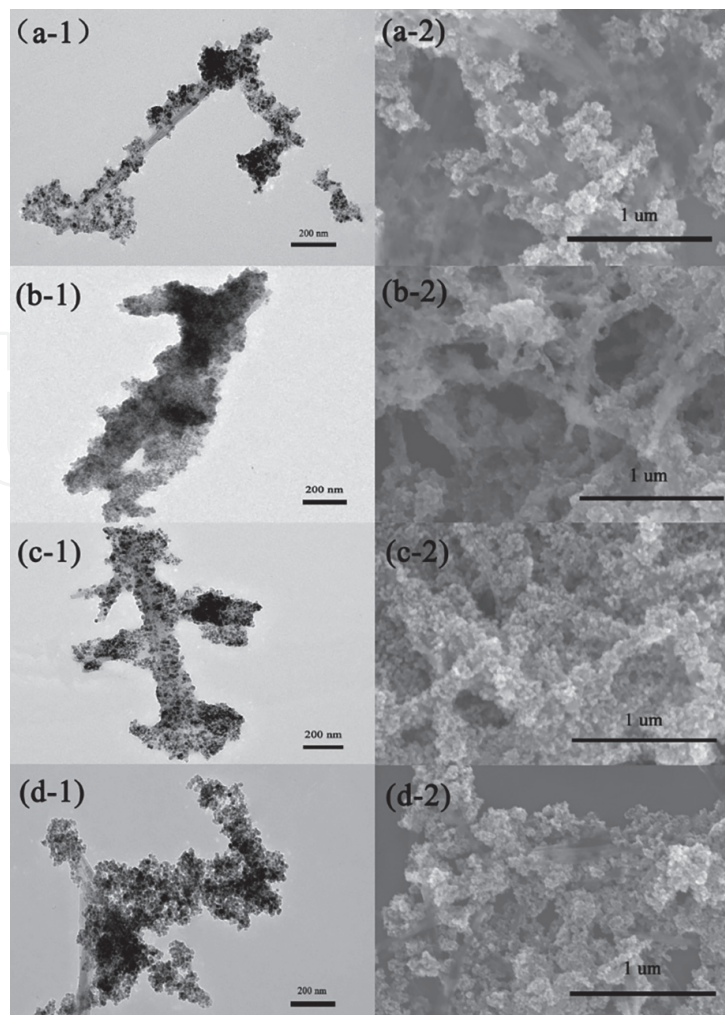


**Figure 10.**  
Images of attapulgites- $\text{Fe}_3\text{O}_4$  one-dimensional nanocomposites synthesized in different temperature: TEM: (a-1) 40°C; (b-1) 60°C; (c-1) 80°C; (d-1) 100°C; SEM: (a-2) 40°C; (b-2) 60°C; (c-2) 80°C; (d-2) 100°C.

### 3.2.4 Effect of mixing method

In the process of synthesizing mineral- $\text{Fe}_3\text{O}_4$  one-dimensional nanocomposites, the stirring mode also has an effect on the uniform deposition of magnetic particles on the surface of one-dimensional nanominerals. **Figure 11** shows the effect of magnetic stirring and electric stirring on the uniform deposition of magnetic particles on the surface of mineral materials. From the TEM in **Figure 11**, it can be seen that a few  $\text{Fe}_3\text{O}_4$  nanoparticles are coated on the surface of the sample prepared by magnetic stirring and most of the sepiolite frameworks are naked (**Figure 11C** and **D**). The  $\text{Fe}_3\text{O}_4$  coated on the surface of sepiolite prepared by electric stirring are more uniform. This is due to the existence of magnetons in the magnetic stirring system, which leads to the aggregation of  $\text{Fe}_3\text{O}_4$  particles on the surface of magnetons and inhibits the deposition of  $\text{Fe}_3\text{O}_4$  particles on the surface of sepiolite nanorods. In addition, the force of magnetic stirring on the sample is relatively weak and the dispersion effect is poor, resulting in less  $\text{Fe}_3\text{O}_4$  nanoparticles on the surface of sepiolite. In the electric stirring system of high stirring speed, the  $\text{Fe}_3\text{O}_4$  particles are uniformly dispersed and the particle size is smaller.

### 3.2.5 Effect of dispersant

In the process of magnetic 1D nanominerals synthesis, there is a problem of agglomeration, so it is necessary to add dispersant. **Figure 12** shows the TEM images



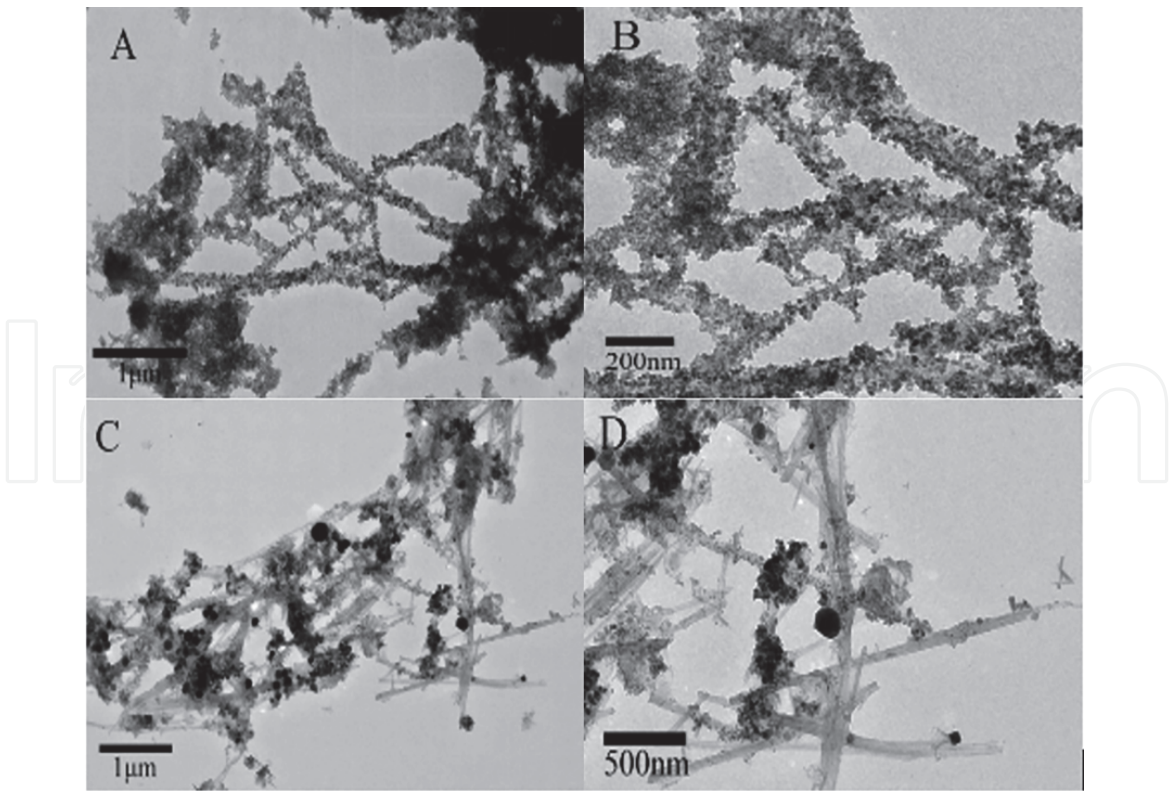


**Figure 11.**  
*Magnetic sepiolite rods prepared by electric stirring (A and B) and magnetic stirring (C and D).*

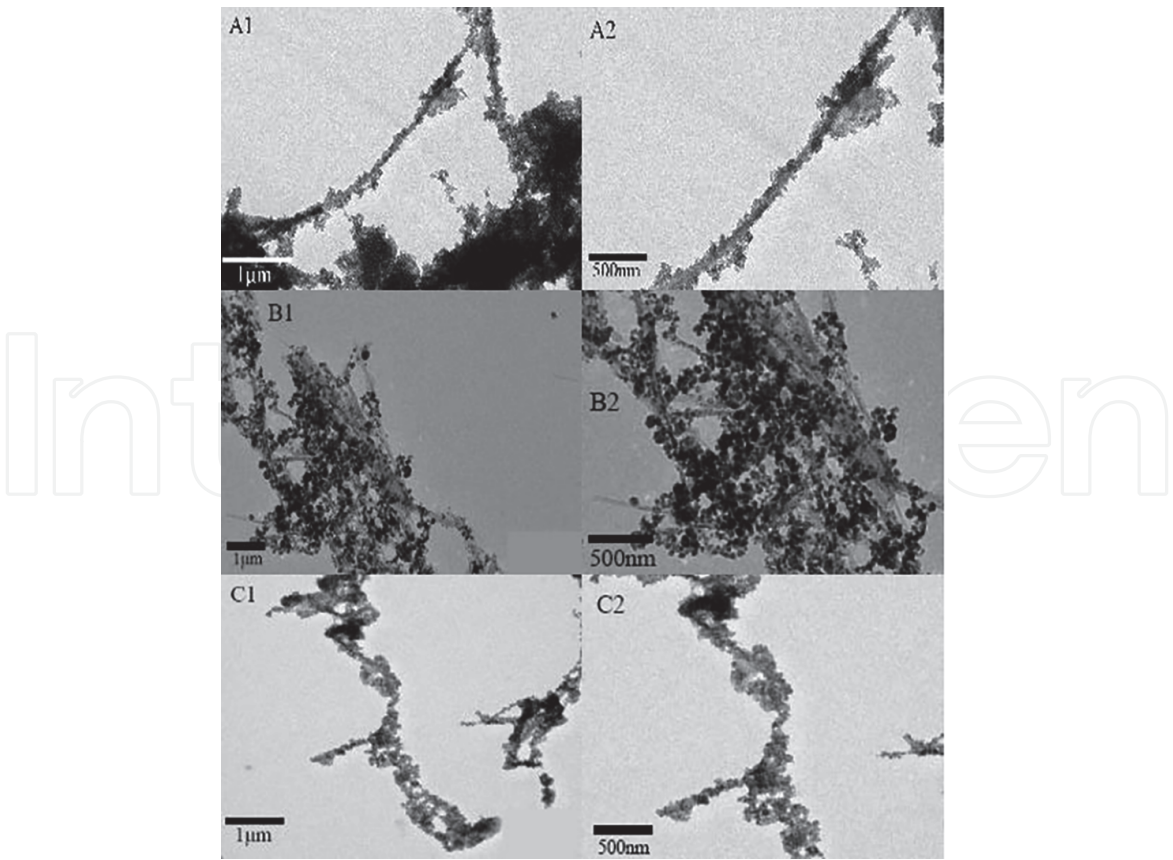


**Figure 12.**  
*TEM of magnetic 1D nanominerals prepared by adding dispersant. A1 and A2: Sepiolite@Fe<sub>3</sub>O<sub>4</sub> without adding dispersant; B1 and B2: Sepiolite@Fe<sub>3</sub>O<sub>4</sub> with organic dispersant; C1 and C2: Sepiolite@Fe<sub>3</sub>O<sub>4</sub> with inorganic dispersant.*

of magnetic 1D nanominerals prepared by adding inorganic/organic dispersant. The results show that the  $\text{Fe}_3\text{O}_4$  nanoparticles decorated on the surface of the sample with ammonium cationic organic dispersant are less and non-uniform, the particle size of  $\text{Fe}_3\text{O}_4$  is large and there is an aggregation between sepiolite nanorods (**Figure 12 A1 and A2**). However, the  $\text{Fe}_3\text{O}_4$  nanoparticles decorated on the surface of the sample with inorganic dispersant is more uniform, the size of  $\text{Fe}_3\text{O}_4$  nanoparticles is smaller and the dispersion between nanorods is more uniform (**Figure 12 C1 and C2**). The inorganic dispersant can be adsorbed on the surface of the 1D magnetic composite and make the composite negatively charged. Through electrostatic repulsion,  $\text{Fe}_3\text{O}_4$  can be coated uniformly and agglomeration can be reduced at the same time. However, ammonium cationic organic dispersants have weak interaction with the composites, resulting in poor dispersion effect.

### 3.3 Preparation of one-dimensional clay mineral magnetic composites

Here, attapulgite and sepiolite are taken as examples to illustrate the method of synthesizing one dimensional clay mineral magnetic composites is feasible.

#### 3.3.1 Preparation of attapulgite@ $\text{Fe}_3\text{O}_4$ one dimensional magnetic composite

The attapulgites,  $\text{Fe}_3\text{O}_4$  nanoparticles and prepared attapulgites@ $\text{Fe}_3\text{O}_4$  one-dimensional nanocomposites were characterized by XRD, SEM, TEM and infrared spectroscopy to evaluate the morphology and structural characteristics [17]. The results are listed in **Figure 13**. **Figure 13(d)** shows the XRD patterns of pure  $\text{Fe}_3\text{O}_4$  nanoparticles, attapulgite samples and attapulgite@ $\text{Fe}_3\text{O}_4$  nanocomposites. Compared with the standard card of  $\text{Fe}_3\text{O}_4$ , the synthesized  $\text{Fe}_3\text{O}_4$  nanoparticles are

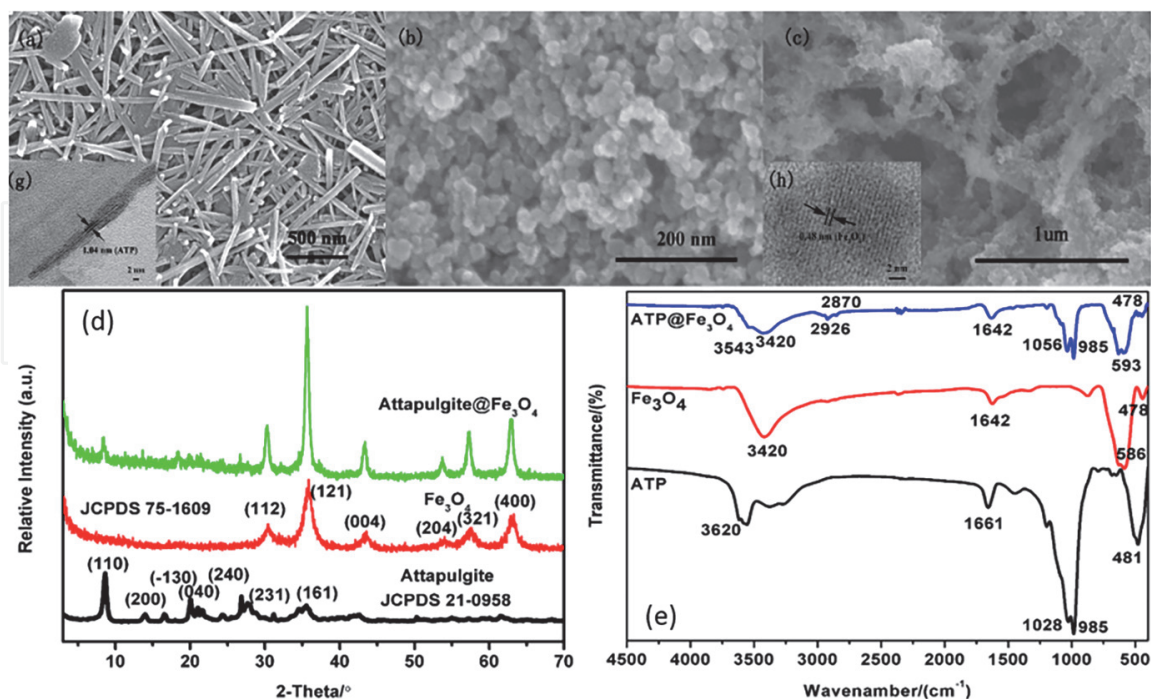


**Figure 13.** Structural characterization of attapulgite,  $\text{Fe}_3\text{O}_4$  and attapulgite@ $\text{Fe}_3\text{O}_4$  nanorods: (a) SEM images of attapulgite; (b) SEM images of  $\text{Fe}_3\text{O}_4$ ; (c) SEM images of attapulgite@ $\text{Fe}_3\text{O}_4$ ; (d) XRD patterns of attapulgite,  $\text{Fe}_3\text{O}_4$  and attapulgite@ $\text{Fe}_3\text{O}_4$ ; (e) FTIR spectra of attapulgite,  $\text{Fe}_3\text{O}_4$  and attapulgite@ $\text{Fe}_3\text{O}_4$  (g) HRTEM image of attapulgite; (h) HRTEM image of attapulgite@ $\text{Fe}_3\text{O}_4$ .



relatively pure with almost no impurity peak. The XRD patterns of attapulgite- $\text{Fe}_3\text{O}_4$  composites correspond well with the standard cards of  $\text{Fe}_3\text{O}_4$  and attapulgite, indicating that attapulgite- $\text{Fe}_3\text{O}_4$  composites can be synthesized by coprecipitation method. **Figure 13(a)–(c)** showed the typical scanning electron microscopy (SEM) images of the pristine attapulgites,  $\text{Fe}_3\text{O}_4$  nanoparticles and attapulgites@ $\text{Fe}_3\text{O}_4$  nanocomposites. **Figure 13(a)** show that the surface of attapulgite is smooth without special impurities. **Figure 13(b)** shows the synthesized pure  $\text{Fe}_3\text{O}_4$  nanoparticles are spherical with a diameter of 10–30 nm. **Figure 13(c)** indicates that the surface of attapulgite is evenly coated with a layer of spherical particles. **Figure 13(g)** shows lattice image of attapulgite by high resolution transmission electron microscope, in which the (110) crystal plane of attapulgite can be found with a spacing of 1.04 nm. Because of the natural production of attapulgite, the crystallinity is low, and the surrounding of attapulgite is wrapped by spherical particles, it is difficult to find the crystal lattice of attapulgite in **Figure 13(h)**. However, there are a lot of new lattice fringes, which are 0.48 nm, and the lattice spacing just corresponds to the (111) plane of  $\text{Fe}_3\text{O}_4$ . The above electronic imaging characterization method show that the nanoparticles coated on the surface of attapulgite are  $\text{Fe}_3\text{O}_4$ . The infrared spectra of attapulgite,  $\text{Fe}_3\text{O}_4$  and attapulgite- $\text{Fe}_3\text{O}_4$  composites are shown in **Figure 13(e)**. The  $1028\text{ cm}^{-1}$  of attapulgite belongs to the stretching vibration of Si-O structure skeleton, and the  $3620\text{ cm}^{-1}$  belongs to the stretching vibration of Al/Mg structure hydroxyl group;  $586\text{ cm}^{-1}$  of  $\text{Fe}_3\text{O}_4$  belongs to the stretching vibration of Fe-O. After the synthesis of attapulgite- $\text{Fe}_3\text{O}_4$  composite, it is found that the wave numbers of Si-O, Al/Mg hydroxyl and Fe-O shifted to  $1056\text{ cm}^{-1}$ ,  $3543\text{ cm}^{-1}$  and  $593\text{ cm}^{-1}$ , respectively, indicating the change of chemical environment of each group. This change directly proved that  $\text{Fe}_3\text{O}_4$  coated on the surface of attapulgite. All results and phenomena above provided the useful information that the  $\text{Fe}_3\text{O}_4$  are successfully bound to the attapulgite uniformly.

### 3.3.2 Preparation of sepiolite@ $\text{Fe}_3\text{O}_4$ one dimensional magnetic composite

In accordance with the method of attapulgite@ $\text{Fe}_3\text{O}_4$  one dimensional magnetic composite, we try to coat the surface of sepiolite with a layer of  $\text{Fe}_3\text{O}_4$

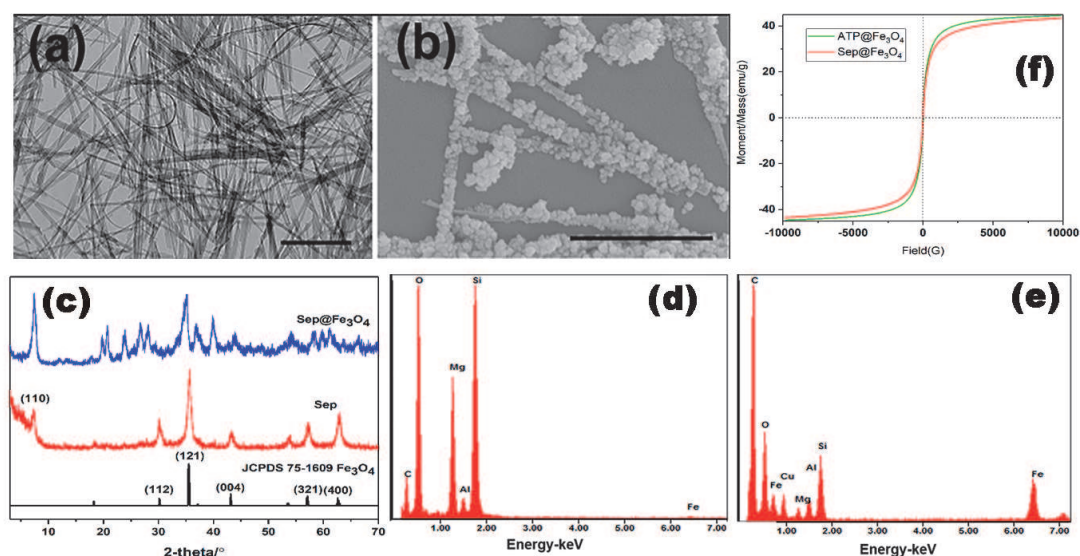


**Figure 14.**

Structural characterization of sepiolite,  $\text{Fe}_3\text{O}_4$  and sepiolite@ $\text{Fe}_3\text{O}_4$  nanorods: (a) SEM images of sepiolite; (b) SEM images of sepiolite@ $\text{Fe}_3\text{O}_4$ ; (c) XRD patterns of sepiolite,  $\text{Fe}_3\text{O}_4$  and sepiolite@ $\text{Fe}_3\text{O}_4$ ; (d) EDS analysis of sepiolite; (e) EDS analysis of sepiolite@ $\text{Fe}_3\text{O}_4$ ; (f) magnetization curves measured at 300 K of one dimensional clay minerals@ $\text{Fe}_3\text{O}_4$ ; ATP: Attapulgite; Sep: Sepiolite.

nanoparticles. The XRD of sepiolite@Fe<sub>3</sub>O<sub>4</sub> composites is shown in **Figure 14(c)**. It can be seen that sepiolite@Fe<sub>3</sub>O<sub>4</sub> samples contain (110) crystal surface of sepiolite and (112), (121), (004), (321) and (400) of Fe<sub>3</sub>O<sub>4</sub>. Thus, sepiolite@Fe<sub>3</sub>O<sub>4</sub> composite can be prepared by the same co-precipitation method with the SEM shown in **Figure 14(b)**. The fiber in **Figure 14(a)** and **(b)** are analyzed by energy spectrum. As shown in **Figure 14(d)**, sepiolite mainly contains Si, Mg and Al elements, and there are a few Fe elements due to the existence of isomorphism. By co-precipitation, spherical particles adhere uniformly and intensively to the surface of sepiolite (**Figure 14(b)**). The energy spectrum analysis of the composite (**Figure 14(e)**) shows that the content of Fe is greatly increased. According to the XRD, the Fe<sub>3</sub>O<sub>4</sub> nanoparticles are wrapped on the outer surface of sepiolite. In conclusion, the co-precipitation method can also be used to uniformly cover the surface of fibrous sepiolite.

### *3.3.3 Magnetic properties of one-dimensional clay mineral magnetic composites*

**Figure 14(f)** shows hysteresis loops of attapulgite@Fe<sub>3</sub>O<sub>4</sub> and sepiolite@Fe<sub>3</sub>O<sub>4</sub> at 300 K, respectively. Both of them are prepared under the same initial ferric salt concentration. Both saturation magnetizations of the obtained samples are about 40 emu/g [16], indicating the magnetic properties of the magnetic composites depend on the content of Fe<sub>3</sub>O<sub>4</sub>. They maintain good superparamagnetism and can timely response to the external magnetic field. It also proves that superparamagnetism can be given to non-magnetic 1D clay minerals by the combination of similar modification and co-precipitation method.

## **4. Construction of sol system with one dimensional magnetic mineral composite**

Due to the large specific surface area and high surface energy, nano materials are easy to agglomerate, which affects the dispersion of nano particles in the substrate material, and further weakens the interaction between particles. Therefore, the dispersion of nanoparticles is the key problem to be solved in the preparation of nano functional materials with excellent performance. The dispersion method of nanoparticles has physical and chemical methods. Physical methods are mainly through mechanical stirring, high-energy acoustic dispersion, high-pressure homogenization and other physical dispersion methods. Chemical methods mainly achieve the stability of the whole dispersion system by adding dispersant, including electrostatic repulsion stabilization mechanism, steric hindrance stabilization mechanism, electrostatic hindrance stabilization mechanism, etc. The selection of solvent is also one of the important factors for the stable dispersion of nano materials. Chemical methods often need the assistance of physical methods to achieve the uniform dispersion of nano materials in the solution. Similarly, for inorganic liquid crystals, the formation of stable colloidal dispersion is the premise of the formation of inorganic liquid crystals.

In this part of the research work, chemical method was used by adding a certain concentration of hydrochloric acid to adjust the ionic strength of the 1D clay mineral@Fe<sub>3</sub>O<sub>4</sub> system. A certain amount of surface charge on the surface of the 1D clay mineral@Fe<sub>3</sub>O<sub>4</sub> form an electric double layer, and preventing the agglomeration of the 1D clay mineral@Fe<sub>3</sub>O<sub>4</sub> nanoparticles through the repulsive force between the electric double layers. With the help of high intensity ultrasound, the whole system is stable.



4.1 Preparation of attapulgite@Fe<sub>3</sub>O<sub>4</sub> colloidal dispersion

4.1.1 Effects of pH

The effect of pH on the dispersion of attapulgite@Fe<sub>3</sub>O<sub>4</sub> in aqueous phase is shown in **Figure 15**. With the decrease of pH, the concentration of hydrochloric acid is increased from 0.0001 mol/L, 0.001 mol/L, 0.005 mol/L, 0.01 mol/L to 0.05 mol/L, the zeta potential of attapulgite@Fe<sub>3</sub>O<sub>4</sub> first increases and then decreases. When the zeta potential of the solution is greater than +30 mV, the nanoparticles reach a stable state. The zeta potential of attapulgite@Fe<sub>3</sub>O<sub>4</sub> is the highest at pH = 3 (+35 mV), which is enough to provide colloidal stability for particles. The zeta potential of attapulgite@Fe<sub>3</sub>O<sub>4</sub> decreases from +35 mV to +27 mV when the pH of the solution decreases from 3 to 2. When the pH of the solution is greater than 3, the zeta potential also decreases sharply. It can be seen that when the pH of the solution is adjusted to 3, the surface charge of attapulgite@Fe<sub>3</sub>O<sub>4</sub> nanoparticles is high enough to provide mutual repulsion force for particle stability, so that the whole system is uniformly dispersed and stable.

4.1.2 The dispersion of attapulgite@Fe<sub>3</sub>O<sub>4</sub> in aqueous phase

Using the method in 4.1.1, the attapulgite@Fe<sub>3</sub>O<sub>4</sub> was dispersed in dilute acid solution with pH = 3. After ultrasonic dispersion for 10 minutes, they could be stored for half a month without obvious sedimentation. Under the optical microscope, the sample is a non-transparent homogeneous liquid, and no particulate matter can be seen by naked eye as shown in **Figure 16(a)**. When attapulgite@Fe<sub>3</sub>O<sub>4</sub> is directly dispersed in water, stable colloidal dispersion cannot be obtained even with long-term ultrasound. Under the optical microscope, a large number of agglomerated composite particles can be seen in the dispersion as shown in **Figure 16(b)**.

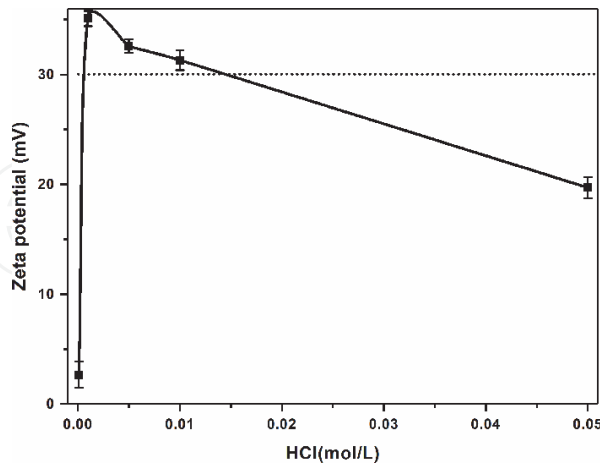


**Figure 15.**  
The relationship between hydrochloric acid concentration and stability of attapulgite@Fe<sub>3</sub>O<sub>4</sub> in water.

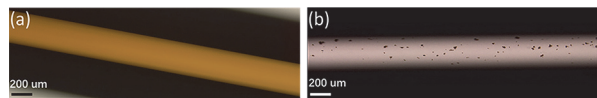


**Figure 16.**  
Optical microscope of attapulgite@Fe<sub>3</sub>O<sub>4</sub> dispersion: (a) the solvent was hydrochloric acid with pH = 3; (b) the solvent was water.

## 4.2 Preparation of sepiolite@Fe<sub>3</sub>O<sub>4</sub> colloidal dispersion

Sepiolite@Fe<sub>3</sub>O<sub>4</sub> was dispersed into dilute acid solution with pH = 3 by the same method as attapulgite@Fe<sub>3</sub>O<sub>4</sub>. The zeta potential of sepiolite@Fe<sub>3</sub>O<sub>4</sub> dispersion was +32 mV. It can exist in the acid solution and form stable colloid.

## 5. Functional properties of one-dimensional magnetic clay mineral sol

### 5.1 Orientation structure comparison of one-dimensional clay mineral@Fe<sub>3</sub>O<sub>4</sub> under magnetic field

When the colloids of one-dimensional clay mineral@Fe<sub>3</sub>O<sub>4</sub> are dripped on the copper mesh and dried naturally under the condition of an external magnetic field, the structure oriented along the magnetic field can be obtained as shown in **Figure 17**. **Figure 17(a)** shows the TEM image of sepiolite@Fe<sub>3</sub>O<sub>4</sub> orientation structure. Sepiolite fiber is a long fiber with an average diameter of 55 nm and an average length of 2.62  $\mu\text{m}$  (**Figure 6**). The diameter of Fe<sub>3</sub>O<sub>4</sub> nanoparticles coated outside is about 20 nm (**Figure 13(b)**). The width of single rod magnetic composite material should be about 100 nm, but the orderly oriented fiber seen from **Figure 17(a)** is 200–600 nm, which indicates that sepiolite@Fe<sub>3</sub>O<sub>4</sub> long fibers tend to aggregate into larger bundles first, and then end-to-end to form longer fiber chains under the magnetic field. The distance between the ordered structures is about 3–4  $\mu\text{m}$ . Attapulgite@Fe<sub>3</sub>O<sub>4</sub> (**Figure 17(b)**) tends to connect single rod with each other. Along the magnetic field orientation, the distance between ordered rods is much closer than sepiolite@Fe<sub>3</sub>O<sub>4</sub>, most of which are below 500 nm. Although sepiolite@Fe<sub>3</sub>O<sub>4</sub> and attapulgite@Fe<sub>3</sub>O<sub>4</sub> have a large number of short-range disordered positions, they are all one-dimensional ordered in the long-range. The different orientation structures of the two 1D clay minerals@Fe<sub>3</sub>O<sub>4</sub> based colloidal dispersions on the copper mesh fully explain the influence of the particle size and morphology of the structural elements on the ordered structure.

### 5.2 Liquid crystal properties of one dimensional magnetic functional mineral

Liquid crystal (LC) has attracted much attention due to its fluidity and birefringence. Its unique anisotropy makes it widely used in TV, notebook computer, mobile phone and other display technologies. Anisotropic nanostructures can be used as structural units to prepare inorganic liquid crystals. Magnetic induced assembly is an effective method to prepare ordered structures. In this part, we will use the magnetic field to induce the orientation of one-dimensional clay mineral@Fe<sub>3</sub>O<sub>4</sub> composites in solution system to prepare ordered materials, and

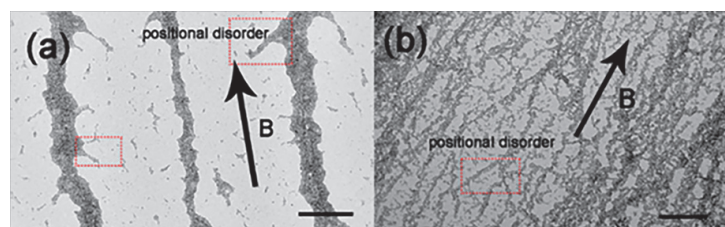


**Figure 17.**  
TEM images of aligned (a) sepiolite@Fe<sub>3</sub>O<sub>4</sub>; (b) attapulgite@Fe<sub>3</sub>O<sub>4</sub>. Scale bars: 1  $\mu\text{m}$ .

discuss the influence of solid content, magnetic field, magnetic field strength, and elemental geometry on their liquid crystal properties.

Attapulgate@Fe<sub>3</sub>O<sub>4</sub> was dispersed in dilute acid solution with pH = 3. After ultrasonic dispersion for 10 minutes, attapulgate@Fe<sub>3</sub>O<sub>4</sub> in dilute acid solution was observed under polarizing microscope. As shown in **Figure 18(a)**, the field of vision is completely dark. Attapulgate@Fe<sub>3</sub>O<sub>4</sub> colloidal dispersion is in isotropic state. Three NdFeB magnets are placed 1 cm away from the sample, and a bright path can be seen in the field of vision (**Figure 18(b)**). When the external magnetic field is removed, the field of vision immediately becomes dark (**Figure 18(c)**). The reversible magnetic response shows that the liquid crystal with birefringent phase controlled by magnetic field can be obtained by coating attapulgate with magnetic particles. Meanwhile, the relaxation time of the liquid crystal is very short within 1 s.

When the particle solid content increased, the colloidal dispersion of attapulgate@Fe<sub>3</sub>O<sub>4</sub> changed from isotropic phase to homogeneous birefringent phase (**Figure 18(d)**) [19]. The light intensity in the polarizing microscope increases gradually, which may be due to the increase of the ordered structure with the increase of the concentration. With the increase of solid content, the color of transmission light in polarizing microscope also changes, which is caused by the color of Fe<sub>3</sub>O<sub>4</sub> nanoparticles.

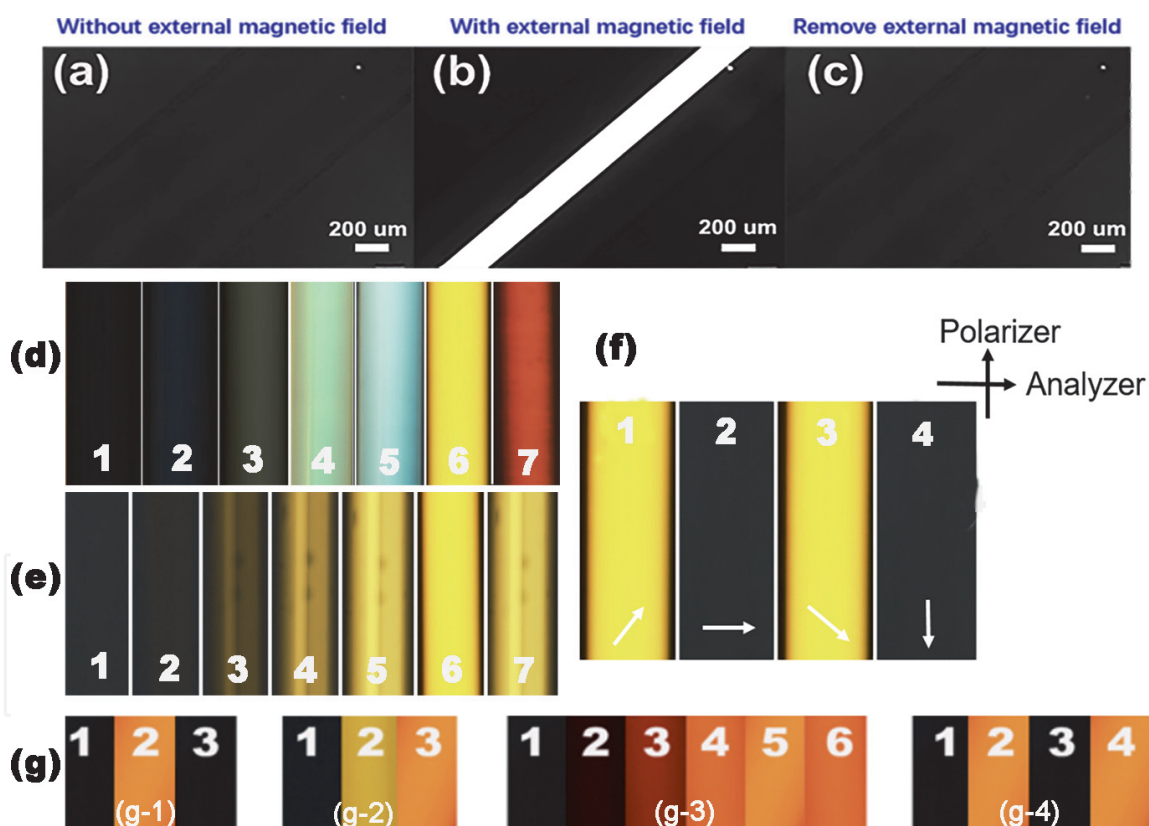


**Figure 18.**

Polarizing microscope of attapulgate@Fe<sub>3</sub>O<sub>4</sub> colloidal dispersion: (a) without magnetic field; (b) adding magnetic field; (c) remove the external magnetic field; (d) different solid content of attapulgate@Fe<sub>3</sub>O<sub>4</sub>: (1) 0.0625 mg/mL; (2) 0.125 mg/mL; (3) 0.25 mg/mL; (4) 0.5 mg/mL; (5) 0.75 mg/mL; (6) 2 mg/mL; (7) 10 mg/mL; (e) polarizing microscope images of attapulgate@Fe<sub>3</sub>O<sub>4</sub> dispersion (2 mg/mL) under different magnetic field intensities: Distance between magnet and sample from left to right: (1) 15 cm; (2) 11 cm; (3) 7 cm; (4) 5 cm; (5) 3 cm; (6) 2 cm; (7) 1 cm; polarizing microscope of attapulgate@Fe<sub>3</sub>O<sub>4</sub> dispersion in different magnetic field directions. The white arrow indicates that the angle between the magnetic field direction and the polarizer direction is: (1) 45°; (2) 90°; (3) 135°; (4) 180°; (g) polarizing microscope of sepiolite@Fe<sub>3</sub>O<sub>4</sub> colloidal dispersion: (g-1): (1) No magnetic field; (2) the distance between the three magnets and the sample is 2 cm; (3) remove the magnetic field; (g-2) samples with different solid contents: (1) 0.0625 mg/mL; (2) 0.5 mg/mL; (3) 2.5 mg/mL (g-3) the distance between the magnet and the sample: (1) 15 cm; (2) 11 cm; (3) 5 cm; (4) 3 cm; (5) 2 cm; (6) 1 cm; (g-4) the angle between the magnetic field direction and polarizer is (1) 0°; (2) 45°; (3) 90°; (4) 135°.



By changing the distance between the NdFeB magnet and the sample, the magnetic field intensity changes, and the liquid crystal transmittance of attapulgite@Fe<sub>3</sub>O<sub>4</sub> shows a high dependence on the magnetic field intensity (**Figure 18(e)**) [19]. With the increase of magnetic field intensity, the transmittance of liquid crystal first increases and then decreases. There is an optimal magnetic field intensity, which makes the order and stability of the whole system reach the best and the optical properties also reach the best.

**Figure 18(f)** shows the effect of the magnetic field direction on the optical properties of the liquid crystal phase [19]. The orientation of attapulgite@Fe<sub>3</sub>O<sub>4</sub> is directly affected by the direction of magnetic field. When the magnetic field is perpendicular or parallel to the polarizer, the whole field of vision is dark. When the angle between the magnetic field and the polarizer is 45°, we can see the strongest transmission light. Changing the direction of magnetic field is equivalent to changing the direction of light. It can be seen that we can control the transmittance of the magnetic controlled liquid crystal by adjusting the direction of the magnetic field.

Using the same method, sepiolite@Fe<sub>3</sub>O<sub>4</sub> was dispersed in dilute acid solution with pH = 3, and the liquid crystal controlled by magnetic field was obtained by ultrasonic dispersion for 10 minutes [16]. As shown in **Figure 18 (g-1)**, it can change from isotropic phase to homogeneous birefringent phase under the magnetic field, and return to isotropic phase after removing the magnetic field. Sepiolite@Fe<sub>3</sub>O<sub>4</sub> based liquid crystal with long fiber structure is similar to attapulgite@Fe<sub>3</sub>O<sub>4</sub> based liquid crystal with short rod structure, and is affected by solid content (**Figure 18 (g-2)**), magnetic field intensity (**Figure 18 (g-3)**) and magnetic field direction (**Figure 18 (g-4)**).

The varied light transmittance of one-dimensional clay minerals@Fe<sub>3</sub>O<sub>4</sub> suspensions are explored between a pair of orthogonal polarizers under external magnetic field. Since the color of the Fe<sub>3</sub>O<sub>4</sub> is reddish brown, the colloidal dispersions absorb the natural white light to a certain extent. It can be seen from **Figure 19** that the colloidal dispersions mainly transmit the visible light with wavelength from 550 to 750 nm [16]. **Figure 19(a)** shows the effect of magnetic field intensity on the transmittance. It can be seen from the figure that at the same concentration, the transmittance of attapulgite@Fe<sub>3</sub>O<sub>4</sub> colloid first increases and then decreases with the increase of magnetic field intensity; The transmittance of sepiolite@Fe<sub>3</sub>O<sub>4</sub> decreases with the increase of magnetic field intensity. The transmittance of attapulgite@Fe<sub>3</sub>O<sub>4</sub> is better than that of sepiolite@Fe<sub>3</sub>O<sub>4</sub>. In order to get the highest transmittance, it is necessary to form a stable ordered structure, and the magnetic

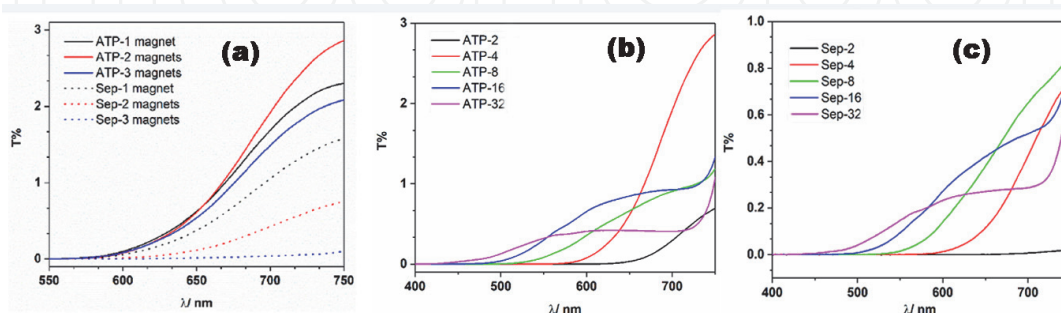


**Figure 19.**

The transmittance of one dimensional clay minerals@Fe<sub>3</sub>O<sub>4</sub> suspension through two crossed polarizers: (a) at 1.0 mg/mL under different magnetic field strength. "Clay-n magnets": n magnets are placed 1 cm away from the sample. (b) by different attapulgite@Fe<sub>3</sub>O<sub>4</sub> solid content with 2 magnets placed 1 cm away from the sample. ATP-2: 2.0 mg/mL; ATP-4: 1.0 mg/mL; ATP-8: 0.5 mg/mL; ATP-16: 0.25 mg/mL; ATP-32: 0.125 mg/mL; (c) with different sepiolite@Fe<sub>3</sub>O<sub>4</sub> solid content by 2 magnets placed 1 cm away from the sample; Sep—Sepiolite. Sep-2: 2.0 mg/mL; Sep-4: 1.0 mg/mL; Sep-8: 0.5 mg/mL; Sep-16: 0.25 mg/mL; Sep-32: 0.125 mg/mL. ATP—Attapulgite; Sep—Sepiolite.



attraction and intermolecular repulsion must reach a balance. There must be a fixed magnetic field for them to get the best optical properties of liquid crystal.

**Figure 19(b)** and **(c)** show the liquid crystal transmittance of attapulgite@Fe<sub>3</sub>O<sub>4</sub> and sepiolite@Fe<sub>3</sub>O<sub>4</sub> under constant magnetic field, respectively. With the increase of concentration, the transmittance first increases and then decreases. The larger the concentration is, the smaller the distance between particles is, and the greater the repulsion is; On the contrary, the smaller the repulsion is. Thus, it will show the law of changing with the concentration in a fixed magnetic field. In the previous discussion, the field of vision is dark under the polarized light microscope when the concentration of one-dimensional clay mineral@Fe<sub>3</sub>O<sub>4</sub> composite is low enough. That is to say, there is no liquid crystal phase even in the presence of magnetic field. It can be inferred that the magnetic controlled liquid crystal prepared by 1D clay minerals is lyotropic liquid crystal, and the liquid crystal phase can be formed only when the concentration requirement is met. The difference of light transmittance between attapulgite@Fe<sub>3</sub>O<sub>4</sub> and sepiolite@Fe<sub>3</sub>O<sub>4</sub> at the same concentration may be caused by the different concentration requirement for the formation of lyotropic liquid crystal, and the result may be related to the structure or properties of the 1D clay mineral itself. In addition, the shorter structure may be easier controlled by magnetic field, forming a more regular ordered structure, showing differences in optical properties. It may be the reason why the transmittance of attapulgite@Fe<sub>3</sub>O<sub>4</sub> based magnetically controlled liquid crystal is slightly better than that of sepiolite@Fe<sub>3</sub>O<sub>4</sub> based magnetically controlled liquid crystal. The influence of Fe<sub>3</sub>O<sub>4</sub> on the transmittance of the system is significant. When the solid content of the system increases, the amount of Fe<sub>3</sub>O<sub>4</sub> particles increases, the absorption of the colloidal system to the light in the low wavelength range increases, resulting in the low transmittance in the low wavelength range; When the solid content decreases, Fe<sub>3</sub>O<sub>4</sub> particles decrease. Although the light transmittance in the high wavelength range decreases, the light transmittance in the low wavelength range increases.

### 5.3 Photonic crystal properties of one dimensional magnetic functional mineral

Colloidal periodic structure formed by self-assembly of monodisperse colloidal structural units is a kind of photonic band gap materials. A new type of photonic band gap material—colloidal magnetic photonic crystal can be formed by adding magnetic components into colloidal structural units. This kind of colloidal magnetic photonic crystal can produce instantaneous response to the magnetic field. Under the magnetic field, the light with a certain frequency in the visible light region can be reflected by the photonic crystal, which makes the photonic crystal show color. This kind of light effect is called Bragg diffraction. By controlling the intensity of external magnetic field, the optical properties of photonic crystal can be easily controlled. In this part, after giving a strong light to the prepared one dimensional magnetic functional minerals colloidal dispersion, the obvious Bragg diffraction can be seen under the external magnetic field, and the influence of magnetic field direction, magnetic field intensity and solid content on the Bragg diffraction effect is discussed.

Attapulgite@Fe<sub>3</sub>O<sub>4</sub> colloidal dispersion is irradiated by a strong light (**Figure 20(a)**). A magnet is used to apply a magnetic field to the colloidal dispersion. As shown in **Figure 20(b)**, bright strong light is reflected by the colloidal dispersion. According to the ordered orientation of the magnetic particles in the magnetic field, it can be inferred that the spacing between the ordered structural units is just comparable to the wavelength of the visible light, so the light in a certain wavelength range is diffracted, and a strong yellow Bragg diffraction light is obtained [19].

The Bragg diffraction light effect of attapulgite@Fe<sub>3</sub>O<sub>4</sub> colloidal dispersion is affected by the magnetic field intensity. As shown in **Figure 21(a)**, with the increase

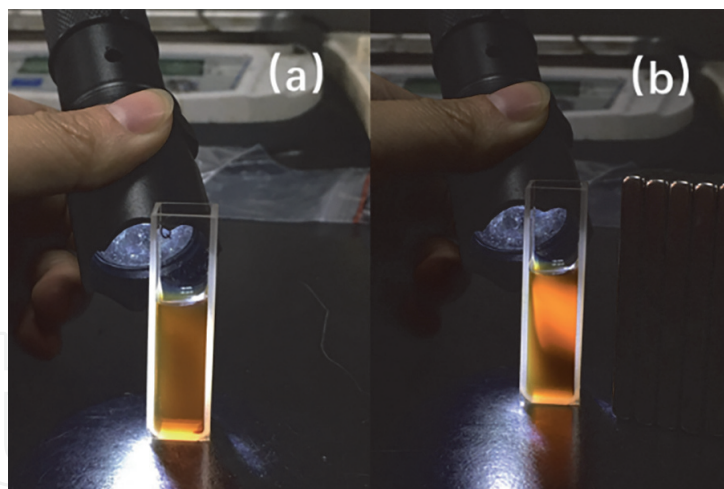


**Figure 20.**  
The optical effects of attapulgite@Fe<sub>3</sub>O<sub>4</sub> colloidal dispersion under strong light: (a) no external magnetic field (b) there is an external magnetic field.

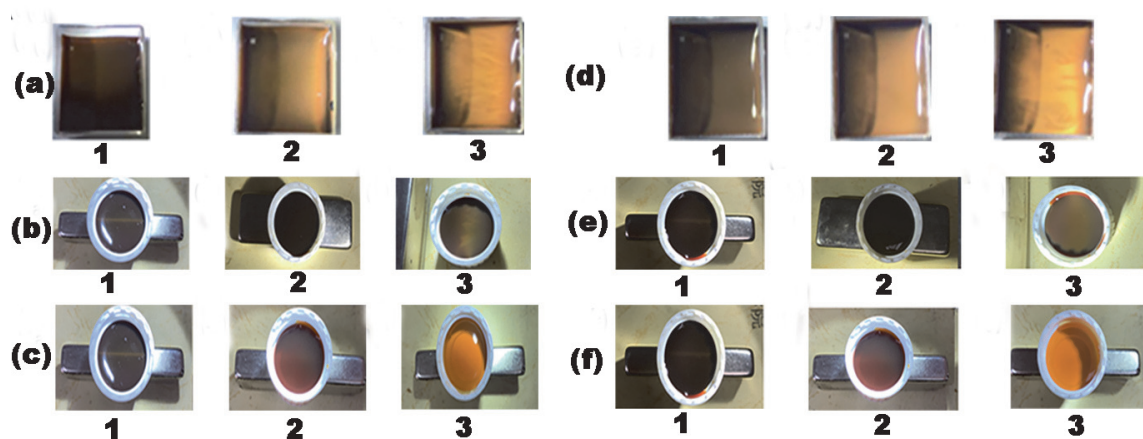


**Figure 21.**  
The light effect of attapulgite@Fe<sub>3</sub>O<sub>4</sub> colloidal dispersion under strong light (a) with the increase of magnetic field intensity: (1) no magnetic field; (2) the distance between the three magnets and the sample is 1 cm; (3) the distance between the three magnets and the sample is 0.2 cm; (b) different directions of magnetic field; (c) different solid contents: (1) 2 mg/mL; (2) 0.5 mg/mL; (3) 0.0625 mg/mL; the optical effects of sepiolite@Fe<sub>3</sub>O<sub>4</sub> colloidal dispersion under strong light (d) with the increase of magnetic field intensity: (1) no magnetic field; (2) the distance between the magnets and sample is 1 cm; (3) the distance between the magnets and sample is 0.2 cm; (e) by the direction of magnetic field; (f) different solid contents: (a) 2 mg/mL; (b) 0.5 mg/mL; (c) 0.0625 mg/mL.

of magnetic field intensity, the intensity of diffraction light gradually increases from (a) to (c). This is related to the regularity of the ordered structure. In a certain range of magnetic field, the larger the magnetic field intensity is, the more regular the ordered structure is formed, and the stronger the Bragg diffraction intensity is.

The optical effect of attapulgite@Fe<sub>3</sub>O<sub>4</sub> colloidal dispersion is affected by the direction of magnetic field under strong light. We adjust the magnetic field direction of the sample by changing the position between the rectangular magnets and the sample as shown in **Figure 21(b)** [16]. When the largest surface of the magnet is perpendicular to the sample (**Figure 21 (b-1)**), only a bright yellow line appears in the middle of the whole circular sample surface. When the largest surface of the magnet is parallel to the sample (**Figure 21 (b-2)**), there is no Bragg diffraction in the whole sample. When the magnet is placed parallel to the sample, a bright yellow band appears in the middle of the sample (**Figure 21 (b-3)**). It can be seen that the orientation of the one dimensional nano magnetic functional minerals is determined by the direction of the magnetic field, which determines if the Bragg diffraction can be formed.

The light effect of attapulgite@Fe<sub>3</sub>O<sub>4</sub> colloidal dispersion under strong light is affected by solid content. As shown in **Figure 21(c)** [16], with the decrease of solid content, the bright Bragg diffraction line in the middle becomes shallower and shallower until it is invisible. Different solid content determines the intermolecular force. Under the same magnetic field, the magnetic field counteracts the intermolecular force, forming different ordered structure spacing, which leads to different Bragg diffraction effect.

The light effect of sepiolite@Fe<sub>3</sub>O<sub>4</sub> colloidal dispersion controlled by magnetic field and solid content under strong light is similar to that of attapulgite@Fe<sub>3</sub>O<sub>4</sub> colloidal dispersion as shown in **Figure 21(d)–(f)** [16].

We drop attapulgite@Fe<sub>3</sub>O<sub>4</sub> colloids and sepiolite@Fe<sub>3</sub>O<sub>4</sub> colloids with different concentrations from 0.00625 mg/mL to 2.0 mg/mL onto the solid substrate, orienting them under the magnetic field, drying them naturally, and observing them under the optical microscope (reflection state) (**Figure 22**). It is found that when the concentration of attapulgite@Fe<sub>3</sub>O<sub>4</sub> is 0.0125 mg/mL, a brilliant rainbow film can be formed on a solid substrate (**Figure 22(a)**). In a certain region, uniform yellow/purple/blue light can be seen and the boundaries of various colors are consistent with the direction of the magnetic field, which proves that the diffraction of the visible light is caused by the ordered structure caused by the magnetic field. However, this phenomenon does not appear in sepiolite@Fe<sub>3</sub>O<sub>4</sub> system at the same concentration (**Figure 22(b)**). It indicated that Bragg diffraction is not only dependent on the solid content, but also on the size of structural elements.

In the previous content, we discussed in detail the microstructures of various magnetic substrates (**Figure 17**). Combined with **Figure 22**, it can be concluded that the solid content and size affect the spacing of ordered structures by influencing the intermolecular force, and then affect the Bragg diffraction of visible light. Although the orientation effect of various 1D clay mineral based magnetic structural elements on the solid base is not equal to the orientation characteristics in the colloidal state, the decisive influence of structure on optical properties is explained from the side. The similar optical effects of attapulgite@Fe<sub>3</sub>O<sub>4</sub> and sepiolite@Fe<sub>3</sub>O<sub>4</sub> indicate the universality of Bragg diffraction effect in 1D clay mineral@Fe<sub>3</sub>O<sub>4</sub> based colloidal dispersion. In the colloidal dispersion system, although the structures of the two 1D clay mineral systems are different, the Bragg diffraction of the two mineral systems are yellow light, and they are also similar under the influence of magnetic field intensity, magnetic field direction and solid content: in a certain range of magnetic field, the greater the magnetic field intensity is, the stronger the Bragg diffraction light is; Different Bragg diffraction regions are obtained in different magnetic field directions; In a certain range of solid content, the Bragg diffraction effect decreases with the decrease of solid content. In the colloidal system, the magnetic field strength and direction determine the magnetic force, while the solid content determines the intermolecular force. The interaction of the two forces

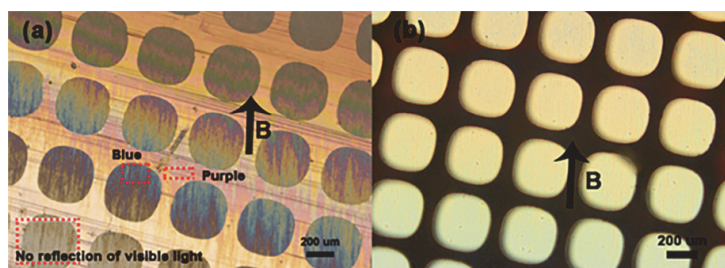


**Figure 22.** Optical microscope images on the substrate (in reflected light): (a) aligned attapulgite@Fe<sub>3</sub>O<sub>4</sub>; (b) aligned sepiolite@Fe<sub>3</sub>O<sub>4</sub>.



determines the orientation structure spacing, and then affects the diffraction effect of the structure on visible light.

6. Application prospect of one-dimensional nano magnetic functional minerals

The similar optical effects of attapulgite@Fe<sub>3</sub>O<sub>4</sub> and sepiolite@Fe<sub>3</sub>O<sub>4</sub> colloidal dispersions under magnetic field indicates that the universality of instant controllable liquid crystal phase and photonic crystal prepared by magnetization of one dimensional clay mineral dispersed in dilute acid solution. Magnetic one

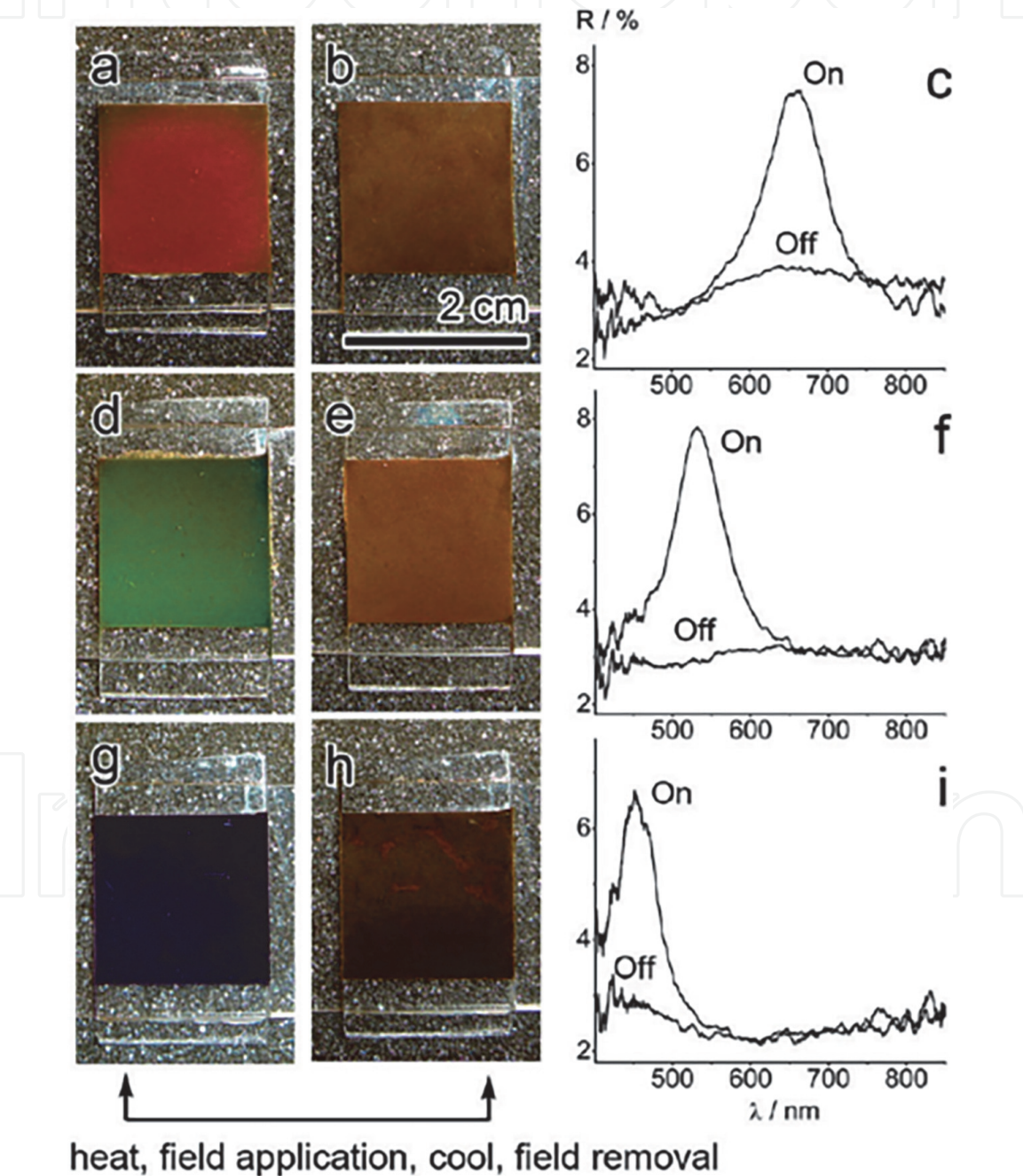


**Figure 23.** Digital photos and reflection spectra of three types of Fe<sub>3</sub>O<sub>4</sub>@SiO<sub>2</sub>/PEGDA microspheres loaded in 1.8 × 1.8 × 0.1 cm<sup>3</sup> glass cells filled with PEG (M<sub>w</sub> = 1500). The diffraction is switched on (a, d, g) or off (b, e, h) by melting the PEG matrix, rotating the microspheres with a magnetic field, and finally cooling down the PEG matrix to lock the sphere orientation. Bistable states can therefore be maintained in the absence of magnetic fields. The corresponding reflection spectra (c, f, i) display diffraction peaks at the “on” stage and none at the “off” stage.

dimensional clay mineral is a material with great potential. Like other common magnetically controlled liquid crystals and photonic crystals, it can be applied in magnetically tunable nanostructures for security and sensing devices, high resolution patterning of multiple structural colors, display device and so on.

Jianping Ge [20] demonstrated a simple switchable color display system in which the color information can be rewritten multiple times by means of a magnetic field using superparamagnetic  $\text{Fe}_3\text{O}_4@\text{SiO}_2$  core/shell particles as shown in **Figure 23**. The matrix material melts when heated, allowing the colors display by

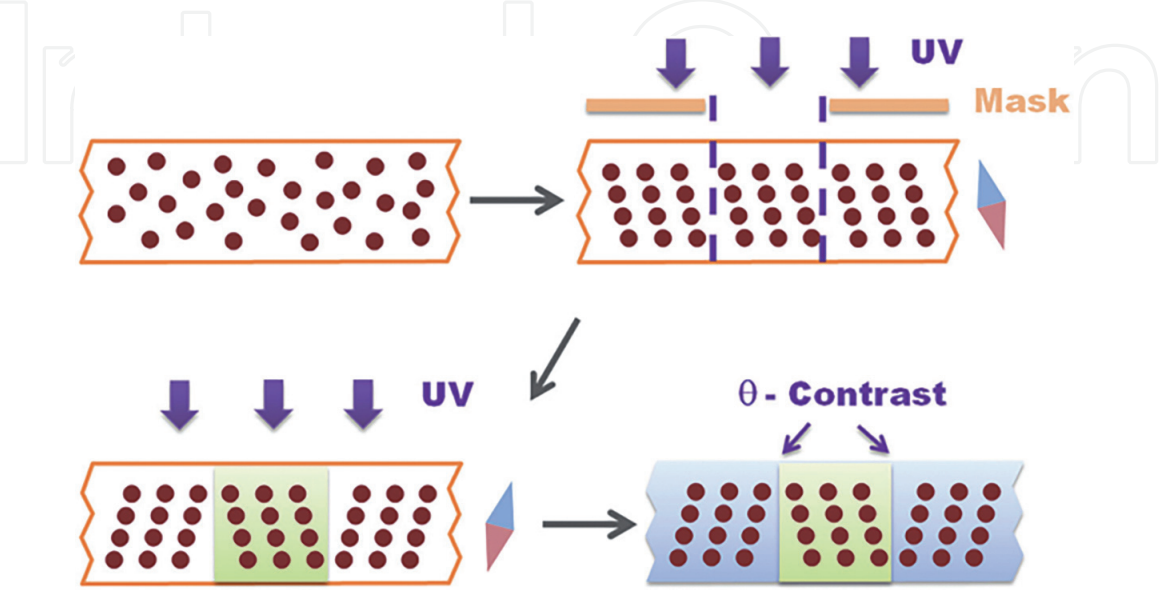


**Figure 24.**  
*Printing process based on the orientational tuning of photonic structures.*



**Figure 25.**  
*Digital photographs of the logo as the incident light is projected from different angles.*

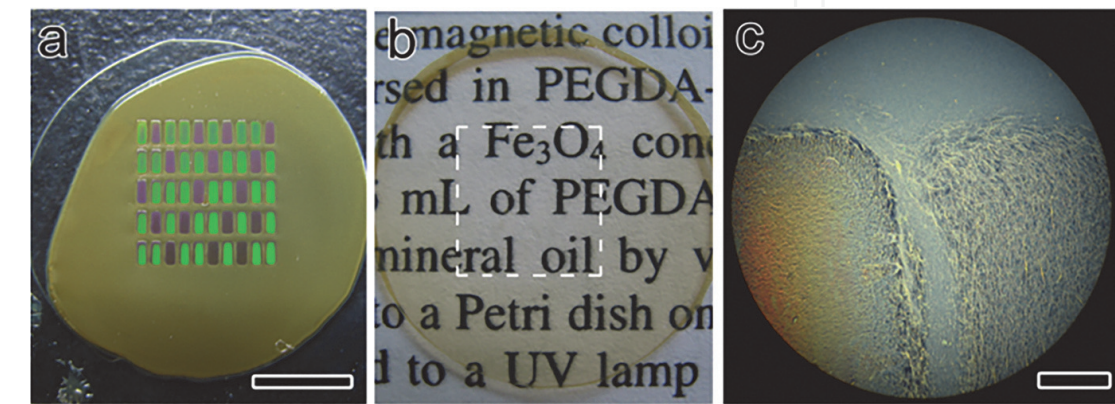


**Figure 26.**  
*(a) Colorimetric binary codes array and (b) an invisible replica printed with an orientational printing process. (c) Optical microscope image of two neighboring code chips in part b. scare bars: (a, b) 5 mm and (c) 200  $\mu\text{m}$ .*



aligning the microspheres under magnetic fields. When the system is cooled to room temperature, the matrix solidifies and the orientation of microspheres is frozen so that the color information remains for a long time without the need of additional energy.

Ruyang Xuan [21] developed a novel photonic printing technique using orientational tuning of photonic structures. In the printing process, the  $\theta$ -contrast pattern is produced by magnetic alignment, orientational tuning, and lithographical photopolymerization (**Figure 24**). When the angle of incident light is changed or samples are tilted, labels printed with two mirror-symmetric or multiple axially symmetric photonic orientations show a switchable color distribution or dynamic color halo (**Figure 25**). This printing method can fabricate colorimetric or invisible codes, which can be decoded by visual observation or a spectrometer (**Figure 26**).

Mingsheng Wang [22] used ferrimagnetic inorganic nanorods as building blocks to prepare liquid crystals (**Figure 27**). The optical properties of the liquid crystals can be instantly and reversibly controlled by manipulating the orientation of the nanorods using considerably weak external magnetic fields (1 mT). They exhibit an

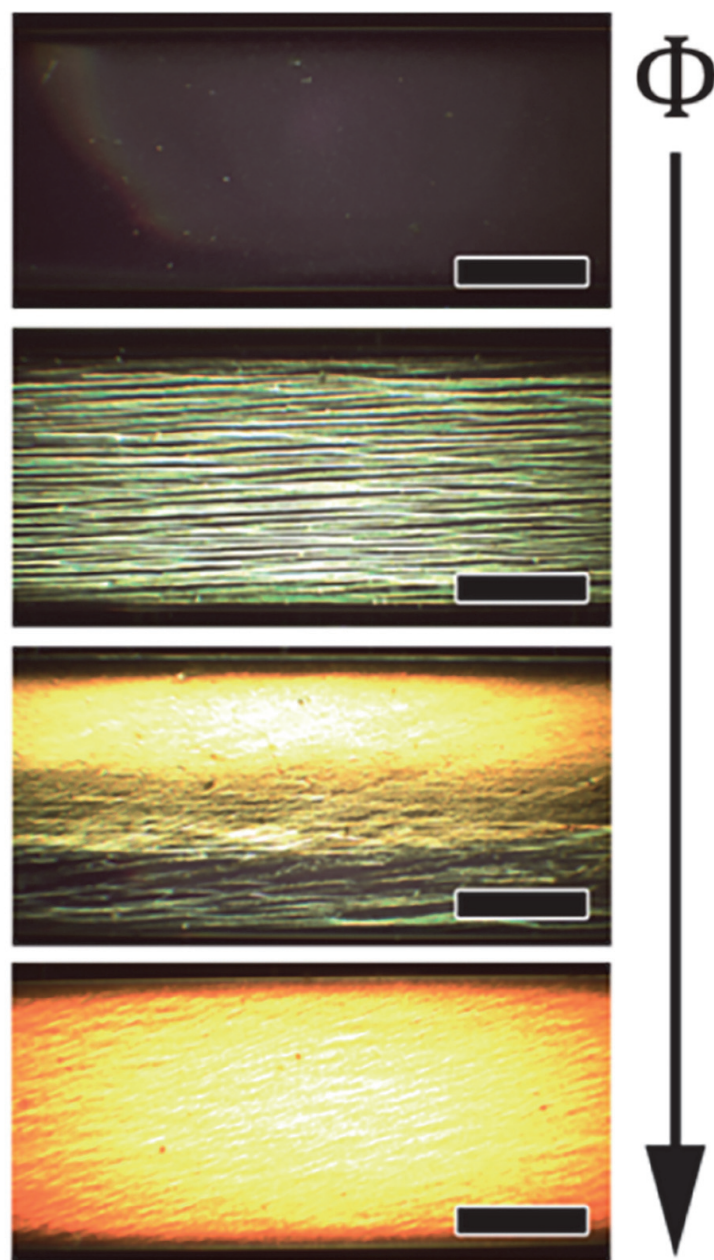


**Figure 27.**  
 POM images of aqueous dispersions of  $\text{Fe}_3\text{O}_4@\text{SiO}_2$  nanorods in a capillary tube at different volume fractions ( $\Phi$ ) of 1%, 3%, 5%, and 10% (from top to bottom). Scale bars: 500  $\mu\text{m}$ .



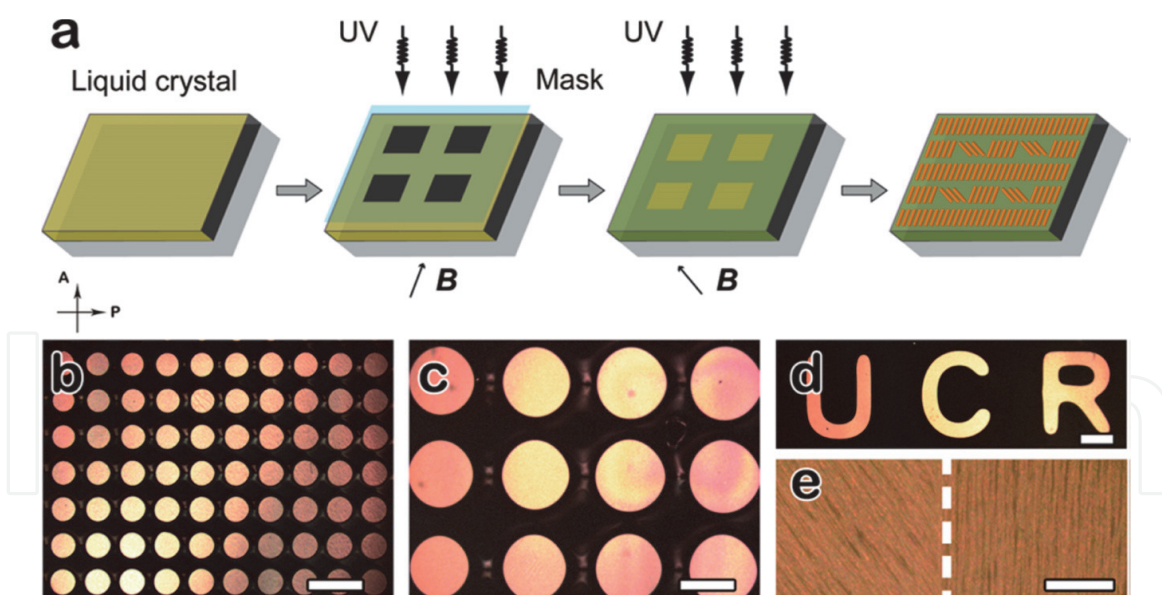


**Figure 28.**

(a) Scheme showing the lithography process for the fabrication of thin films with patterns of different polarizations; (b-d) POM images of various polarization-modulated patterns; (e) enlarged OM image shows the arrangement of nanorods in the pattern (left) and surrounding area (right). Scale bars: (b – d) 500  $\mu\text{m}$ ; (e) 10  $\mu\text{m}$ .

optical switching frequency above 100 Hz under an alternating magnetic field. It is comparable to the performance of commercial liquid crystals using electrical switching. By combining magnetic alignment and lithography processes, it is also possible to create patterns of different polarizations in a thin composite film and control over the transmittance of light in particular areas (**Figure 28**). Developing such magnetically responsive liquid crystals opens the door toward various applications, which may benefit from the instantaneous and contactless nature of magnetic manipulation.

## 7. Conclusion and outlook

This chapter mainly describes the related research of one-dimensional nano clay minerals in the field of optics, including the following four parts: The first part is the composition, structure and properties of one-dimensional nano clay minerals; The second part is the magnetic assembly of one-dimensional nano clay minerals represented by halloysite and sepiolite; The third part is how to prepare colloidal dispersion based on one-dimensional magnetically assembled nano clay minerals; The fourth part is about the liquid crystal properties and photonic crystal properties of magnetic one-dimensional nano clay mineral matrix composites and their application prospects. One dimensional nano clay minerals show great development potential in the field of security and sensing devices, high resolution patterning of multiple structural colors, display device etc., but in the process of research, there are mainly five problems: (1) A broader system stability should be established so that magnetic one dimensional nano clay minerals have a strong stability in a wider pH range, which is conducive to the practical application of materials; (2) Better optical properties need to be obtained by better coating form and more regular coating; (3) It is possible to obtain better Bragg diffraction effect and realize the full range control of the visible region by synthesizing the structural elements with uniform particle size; (4) The magnetic particles coated on the surface of one-dimensional nano clay minerals are easy to fall off; (5) The color of liquid crystal

formed by one-dimensional magnetic nano clay mineral colloid is limited by the color of  $\text{Fe}_3\text{O}_4$ . In the future, researchers can try to synthesize one-dimensional nano clay minerals with more uniform size instead of natural production, so that the magnetic colloidal system could have more regular building blocks. Try other electrolytes or solvents to get more stability of colloidal system. Therefore, there is still a long way to go for one-dimensional nano clay minerals to realize industrial application in optical field.

## Acknowledgements

This work was supported by the Maoming Science and Technology Plan Project (2020580) and the Project of Talents Recruitment of Guangdong University of Petrochemical Technology.

## Conflict of interest

The authors declare no conflict of interest.

## Author details


Meng Fu<sup>1\*</sup>, Zepeng Zhang<sup>2</sup>, Rui Jiang<sup>2</sup> and Hongbao Liu<sup>2</sup>

<sup>1</sup> School of Materials Sciences and Technology, Guangdong University of Petrochemical Technology, Maoming, China

<sup>2</sup> Beijing Key Laboratory of Materials Utilization of Nonmetallic Minerals and Solid Wastes, National Laboratory of Mineral Materials, School of Materials Science and Technology, China University of Geosciences, Beijing, China

\*Address all correspondence to: [fumeng19930731@163.com](mailto:fumeng19930731@163.com)

## IntechOpen

© 2021 The Author(s). Licensee IntechOpen. This chapter is distributed under the terms of the Creative Commons Attribution License (<http://creativecommons.org/licenses/by/3.0>), which permits unrestricted use, distribution, and reproduction in any medium, provided the original work is properly cited. 

## References

- [1] Li XZ, Shi HY, Zuo SX, et al. Lattice reconstruction of one-dimensional mineral to achieve dendritic heterojunction for cost-effective nitrogen photofixation. *Chemical Engineering Journal*. 2021. DOI: 10.1016/j.cej.2021.128797.
- [2] Pei ML, Pan CG, Wu Dan, et al. Surface hydrophilic-hydrophobic reversal coatings of polydimethylsiloxane-palygorskite nanosponges. *Applied Clay Science*. 2020. DOI: 10.1016/j.clay.2020.105546.
- [3] Papoulis D, Somalakidi K, Todorova N, et al. Sepiolite/TiO<sub>2</sub> and metal ion modified sepiolite/TiO<sub>2</sub> nanocomposites: synthesis, characterization and photocatalytic activity in abatement of NO<sub>x</sub> gases. *Applied clay science*. 2019. DOI: 10.1016/j.clay.2019.105156.
- [4] Tang J, Mu B, Zong L, et al. Facile and green fabrication of magnetically recyclable carboxyl-functionalized attapulgite/carbon nanocomposites derived from spent bleaching earth for wastewater treatment. *Chemical Engineering Journal*. 2017; 322: 102-114. DOI: 10.1016/j.cej.2017.03.116.
- [5] Li LX, Li BC, Fan L, et al. Palygorskite@Fe<sub>3</sub>O<sub>4</sub>@polyperfluoroalkylsilane Nanocomposites for Superoleophobic Coatings and Magnetic Liquid Marbles. *Journal of Materials Chemistry A*. 2016; 16: 5859-5868. DOI: 10.1039/C6TA00758A.
- [6] Ren HD, Wang S, Lian W, et al. Preparation of Coral-like Palygorskite-dispersed Fe<sub>3</sub>O<sub>4</sub>/polyaniline with Improved Electromagnetic Absorption Performance. *Applied Clay Science*. 2021. DOI: 10.1016/j.clay.2021.106009.
- [7] Zhu J, Zhou S, Li M, et al. PVDF mixed matrix ultrafiltration membrane incorporated with deformed rebar-like Fe<sub>3</sub>O<sub>4</sub>-palygorskite nanocomposites to enhance strength and antifouling properties. *Journal of Membrane Science*. 2020. DOI: 10.1016/j.memsci.2020.118467.
- [8] Ruiz-Hitzky E, Darder M, Alcántara ACS, et al. Recent Advances on Fibrous Clay-Based Nanocomposites. In: Kalia S, Haldorai Y, editors. *Organic-Inorganic Hybrid Nanomaterials. Advances in Polymer Science*. Springer; 2014. p. 39-86. DOI: 10.1007/12\_2014\_283.
- [9] Chen LF, Liang HW, Lu Y, et al. Synthesis of an attapulgite clay@carbon nanocomposite adsorbent by a hydrothermal carbonization process and their application in the removal of toxic metal ions from water. *Langmuir the Acs Journal of Surfaces & Colloids*. 2011; 27: 8998-9004. DOI: 10.1021/la2017165.
- [10] Yuan M, Gao G, Hu X, et al. Premodified Sepiolite Functionalized with Triethylenetetramine as an Effective and Inexpensive Adsorbent for CO<sub>2</sub> Capture, *Industrial & Engineering Chemistry Research*. 2018; 57: 6189-6200. DOI: 10.1021/acs.iecr.8b00348.
- [11] Yuan B, Yin XQ, Liu XQ, et al. Enhanced Hydrothermal Stability and Catalytic Performance of HKUST-1 by Incorporating Carboxyl-Functionalized Attapulgite. *Acs Applied Materials & Interfaces*. 2016; 8: 16457-16464. DOI: 10.1021/acsami.6b04127.
- [12] Corma A, Fornés V, Mifsud A, et al. Aluminum-Exchanged Sepiolite as a Component of Fluid Cracking Catalysts. *Acs Symposium Series*. 1991; 293-307. DOI: 10.1021/bk-1991-0452.ch018.
- [13] Zhuang G, Zhang Z, Jaber M, et al. Comparative study on the structures



and properties of organo-montmorillonite and organo-palygorskite in oil-based drilling fluids. *Journal of Industrial & Engineering Chemistry*. 2017; 56: 248-257. DOI: 10.1016/j.jiec.2017.07.017.

[14] Wang AQ, Wang WB, Zheng YA, et al. *Attapulgite Rod Bundle Dissociation and its Nano Functional Composites*. Beijing, 2014. ISBN: 978-7-03-041706-0.

[15] Shan Q. *Structure Mineralogy*. Beijing, 2011. ISBN: 978-7-301-16157-9/P-0073.

[16] Fu M, Li XM, Zhang ZP. Comparative study of optical properties by clay minerals with magnetic coating in colloidal dispersion under an external magnetic field. *Applied Clay Science*. 2019; 181. DOI: 10.1016/j.clay.2019.105224.

[17] Fu M, Li XM, Jiang R, et al. One-dimensional Magnetic Nanocomposites with Attapulgites as Templates: Growth, Formation Mechanism and Magnetic Alignment, *Applied Surface Science*. 2018; 441: 239-250. DOI: 10.1016/j.apsusc.2018.02.028.

[18] Jiang R, Zhang ZP, Chen HW, et al. Preparation of one-dimensional magnetic nanocomposites with palygorskites as templates after inorganic modification, *Colloids and Surfaces A: Physicochemical and Engineering Aspects*. 2021. DOI: 10.1016/j.colsurfa.2021.126520.

[19] Fu M, Zhang ZP. Highly Tunable Liquid Crystalline Assemblies of Superparamagnetic rod-like Attapulgite@Fe<sub>3</sub>O<sub>4</sub> nanocomposite. *Materials Letters*. 2018; 226: 43-46. DOI: 10.1016/j.matlet.2018.04.128.

[20] Ge JP, Lee H, He L, et al. Magnetochromatic Microspheres: Rotating Photonic Crystals. *Journal of the American Chemical Society*. 2009;

131:15687-15694. DOI: 10.1021/ja903626h.

[21] Xuan RY, Ge JP. Photonic printing through the orientational tuning of photonic structures and its application to anticounterfeiting labels. *Langmuir the Acs Journal of Surfaces & Colloids*. 2011; 27: 5694-5699. DOI: 10.1021/la200571y.

[22] Wang MS, He L, Zorba S, et al. Magnetically actuated liquid crystals. *Nano Letters*. 2014; 14: 3966-3971. DOI: 10.1021/nl501302s.